CHARACTERIZATION OF THE *STAPHYLOCOCCUS AUREUS* NITRIC OXIDE SYNTHASE GENE AND ITS ROLE IN BIOFILM DEVELOPMENT

By

ERIN AHMO ALMAND

A THESIS PRESENTED TO THE GRADUATE SCHOOL
OF THE UNIVERSITY OF FLORIDA IN PARTIAL FULFILLMENT
OF THE REQUIREMENTS FOR THE DEGREE OF
MASTER OF SCIENCE

UNIVERSITY OF FLORIDA

2010

To my husband, family, and lab mates

ACKNOWLEDGMENTS

First and foremost, I thank my parents, Carey Anne and Timothy, for always supporting me, regardless of the ridiculousness of my endeavors. In addition, I thank my brother and sister-in-law, Ryan and Amanda, for bringing me back to reality when I needed it. I thank my Professor, Dr. Rice, for taking a chance and letting me into her lab despite knowing basically nothing about me. The lab would have been nothing without my lab mates, which I thank for helping me to adjust to graduate student life and making it a joy to go to work every day. For sharing in my strife and those giggly nights over Woodchuck, I thank my roommate, Robin, for helping me get through University of Florida and being there so I would not have to hack it alone. I thank the Air Force Institute of Technology for this wonderful opportunity. For their assistance and great ideas I thank my committee members, Dr. K.T. Shanmugam and Dr. Graciela Lorca. Furthermore, I thank my collaborators, Dr. Richardson and Dr. Bayles for their help with the project. Last, but certainly not least, I thank my husband, Austin, for being my inspiration and providing me with the drive and motivation I needed to finish this degree.

TABLE OF CONTENTS

page

LIST OF TABLES

LIST OF FIGURES

Abstract of Thesis Presented to the Graduate School
of the University of Florida in Partial Fulfillment of the
Requirements for the Degree of Master of Science

CHARACTERIZATION OF THE *STAPHYLOCOCCUS AUREUS* NITRIC OXIDE SYNTHASE GENE AND ITS ROLE IN BIOFILM DEVELOPMENT

By

Erin Ahmo Almand

December 2010

Chair: Kelly C. Rice
Major: Microbiology and Cell Science

Nitric oxide (NO) is emerging as a ubiquitous signaling molecule that plays a role in bacterial biofilm development. For example, in *Pseudomonas aeruginosa*, endogenous NO production via anaerobic respiration promotes cell death and dispersal during biofilm development. One of the potential sources of endogenous NO in *Staphylococcus aureus* is a bacterial NO-synthase (SaNOS). Data published by other groups have shown that purified SaNOS converts L-arginine to citrulline and NO, and a *S. aureus* strain defective in the NO synthase (*nos*) gene has been reported to have increased sensitivity to oxidative stress during planktonic growth, similar to results reported for the *Bacillus subtilis nos* mutant. However, the contribution of NOS to *S. aureus* biofilm growth is yet to be elucidated. Quantitative reverse-transcriptase PCR (qRT-PCR) analysis of RNA isolated from *S. aureus* UAMS-1 has demonstrated that expression of the *nos* gene (SAR2007 of the MRSA252 genome, NC_002952.2) is up-regulated during low-oxygen growth relative to aerobic growth, and that *nos* is co-transcribed with a downstream SAR2008 gene, a putative prephenate dehydratase. Furthermore, published RNA microarray data has shown that *nos* expression is up-regulated in the presence of hydrogen peroxide (H_2O_2), and these results were

confirmed in this study by qRT-PCR analysis of RNA isolated from UAMS-1 cultures grown in the presence and absence of H_2O_2. Strain UAMS-1 and an isogenic *nos* polar insertion mutant displayed comparable growth in both TSB and biofilm media under planktonic growth conditions. However, when grown on a TSA plate there was increased pigmentation in the *nos* mutant which corresponds to an increase in *nos* expression as monitored by a *nos* promoter-GFP reporter plasmid construct. Phenotypic differences were also observed when UAMS-1 and the *nos* mutant were grown as static biofilms. The *nos* mutant had a more attached structure when compared to the UAMS-1 wild-type strain, which, when analyzed by COMSTAT software, showed an increase in biomass and average thickness in the *nos* mutant. Analysis also showed a decrease in biomass to surface area ratio, suggesting the *nos* mutant biofilm may be less adaptable to a changing environment compared to the wild-type UAMS-1. Complementation of the *nos* mutation resulted in reversion of the pigment production, biofilm phenotypes and qRT-PCR data back to wild-type results. Based on these results and the link between SaNOS and oxidative stress, a working model is proposed in which *nos* expression may be up-regulated in *S. aureus* biofilms in response to oxidative stress (such as in the presence of immune cell respiratory burst), which in turn enhances endogenous NO production in the biofilm which may participate in regulatory processes such as signaling cell dispersal.

CHAPTER 1
INTRODUCTION

Staphylococcus aureus

Staphylococcus aureus is a spherical Gram-positive bacterium arranged in grape-like clusters [1] with a 2800 kbp chromosome supplemented with prophages, plasmids and transposons [2,3]. *S. aureus* is a facultative anaerobe which can grow via aerobic respiration, anaerobic respiration and mixed acid fermentation, allowing its persistence under a variety of growth conditions, including a sessile, biofilm lifestyle. The alteration of this metabolism has phenotypic effects, with the main difference being virulence. Anaerobically, the TCA cycle is down regulated and transcription of virulence factors is decreased in favor of supporting the growth of the microbe [4]. *S. aureus* also has a golden pigment resulting from carotenoid production, which acts as an antioxidant defense mechanism and allows for protection against oxidant-based clearance of host innate immune system-released reactive oxygen species such as hydrogen peroxide (H_2O_2) and hypochlorite [5].

While carotenoid pigment may help *S. aureus* to some degree in terms of avoiding the immune system, it is only one of a plethora of bacterial factors which make *S. aureus,* and more specifically Methicillin-Resistant *Staphylococcus aureus* (MRSA), the leading cause of death by a single infectious agent and the leading cause of human bacterial infections worldwide [6]. The infectious capabilities of *S aureus* are in part due to its transmission in a variety of ways, including crowding, skin to skin interactions with healthy or already compromised skin (wounds), contaminated surfaces or a lack of cleanliness in general [6]. *S. aureus* can cause a number of infections, in all tissues and organ systems, with the more common diseases being bacteremia, endocarditis,

sepsis, toxic shock, and necrotizing fasciitis [1]. While the number of diseases caused by *S. aureus* is alarming, the main reason for its prevalence and severity of disease is a variety of virulence factors (Table 1-1) and its multi-drug resistance capabilities, including benzyl penicillin (beta lactamase activity), methicillin (*mecA*) and even vancomycin (*vanA*) resistance [7,8,9].

These multiple resistance strains fall into two categories, hospital acquired methicillin resistant *S. aureus* (HA-MRSA) and community acquired methicillin resistant *S. aureus* (CA-MRSA). HA-MRSA infects individuals with a predisposition to infection, whether they are immunocompromised or have an implanted device such as a catheter or intravenous (IV) line. In contrast, CA-MRSA infects seemingly healthy individuals, although there is a dispute as to whether or not there is an actual growth advantage in some strains allowing for easier colonization or, potentially, an unidentified factor in the hosts making individuals more susceptible [7].

Virulence Regulation

Virulence regulation is a wide area of study, especially when attempting to determine therapeutics for *S. aureus.* Regulation occurs through a variety of signals in response to the host, environment, growth phase, adhesion redundancy, presence of exotoxins and the presence of proteases [10]. There are two main groups of regulators, the two-component systems and the other regulators. A widely studied example of a two-component system is *agrBDCA* (accessory gene regulator), which is a quorum sensing system responsible for regulation of biofilm formation (discussed in more detail below), virulence gene expression and detachment [11]. It regulates virulence gene expression by down-regulating cell surface adhesions during stationary phase, or in response to high cell density, and simultaneously up-regulating secreted virulence

factors and toxins [12]. It is made up of two primary transcripts designated RNA II and RNA III, from the promoters P2 and P3, respectively. P2 makes up a four gene operon encoding the AgrBDCA proteins. AgrB is a transmembrane protein involved in processing AgrD into an octopeptide which is then secreted as an autoinducing peptide (AIP) signal [13]. AgrA and AgrC are members of a two-component system where AgrC is the histidine kinase that binds the AIP and AgrA is its corresponding response regulator [14]. Binding of AIP to AgrC induces subsequent phosphorylation of AgrA, which in turn allows binding to the P3 promoter region and up-regulation of the P3 transcript. The P3 transcript encodes the effector of the *agr* system, RNAIII, which is an untranslated regulatory RNA molecule, that determines the expression of target genes at either the transcriptional or translational level[14]. The expression and regulation of virulence genes play a large role in the interaction between *S. aureus* and the immune system.

Biofilms

A biofilm is a microbial community enveloped by an extracellular matrix adhered to a solid surface and each other. There are multiple reasons why bacteria may choose this sessile lifestyle in lieu of a motile or planktonic state, such as the ability to coordinate activities through intercellular signaling, a variance in metabolic activities leading to potential defense strategies, and for pathogens, to increase the persistence of infection within a host [15]. There are three main stages of biofilm development: attachment, maturation and dispersal (Figure 1-1). Attachment is the initial colonization of the surface, and is affected by a variety of factors to include surface conditioning (accumulation of nutrients at the surface fluid interface [16]), mass transport (mechanism by which bacteria are transported to the surface to colonize [17]), surface

charge (the charge on the cell surface compared to the charge on the colonizing surface [18]), hydrophobicity (of the surface and of the corresponding bacterial attachment factors[19]) and microtopography (surface cracks and crevices which may better allow for cell attachment [20]) [21]. Maturation is the next stage, which is characterized by an increase in biomass, production of a protective extracellular polysaccharide and/or protein-based biofilm matrix, and the formation of various structures such as towers. Current research has also shown that extracellular genomic DNA (eDNA) release plays a large role in attachment as well as in biofilm maturation in a number of different bacteria [22-31]. It is released by autolysis of bacterial cells and acts as an adhesive. Last is dispersal, the portion of the life cycle which allows microcolonies to detach and promote biofilm formation in previously uncolonized areas. Dispersal is mediated by several factors such as environmental conditions, changing oxygen levels, nutrient depletion, changing nutrient composition, increased protease activity and increased concentration of quorum sensing signals [22].

Staphylococcus aureus **Biofilms**

Staphylococcus aureus biofilms are very difficult to eradicate and have a high probability of disseminating to other sites in the body [23]. They have the same three stages of development as described above (attachment, maturation and dispersal), with specific cell signals occurring at each stage. Regulated cell lysis and the release of eDNA is of particular importance in *S. aureus* biofilms [24]. This eDNA is important for biofilm adhesion in vitro, especially within the first four hours of colonization [24,25]. During this initial colonization period is also when *S. aureus* initially binds to human matrix proteins, such as fibrinogen and fibronectin, via microbial surface components recognizing adhesive matrix molecule (MSCRAMMS) [26]. These molecules have a

exposed binding domain for interaction with the host, a cell-wall spanning domain, and a domain for covalent or noncovalent attachment to bacterial surfaces [26]. A recent study suggests that several of these MSCRAMMS, specifically fibrinogen and fibronectin-binding proteins (FnBPA and FnBPB, respectively), are important for biofilm attachment in MRSA strains, but not in MSSA strains, suggesting that the contribution of certain MSCRAMMS towards biofilm development may be strain dependent [27]. Overall, initial colonization sets the stage for biofilm growth and development.

Maturation

After this initial adherence, polysaccharide intercellular adhesion (PIA) and the extracellular matrix are produced. This production is mediated by the *icaADBC* locus and is increased under anaerobic environments [4,28]. IcaA is an N-acetylglucoaminyltransferase while IcaC and IcaD are membrane associated proteins which chaperone IcaA. IcaB is the enzyme responsible for deacetylation of N-acetyl glucosamine. This operon is repressed by IcaR which binds upstream of the *ica* start codon [28]. While this polysaccharide production plays a large role in biofilm formation in some *S. aureus* strains, there is a large proportion of them which do not require PIA for biofilm formation [29]. Dispersin B is a glycoside hydrolase enzyme (produced by the pathogen *Aggregatibacter actinomycetemcomitans*) capable of removing the biofilms which are PIA dependent [30]. However, many other staphylococcal biofilms were found to be unaffected by this treatment [22,30]. Rather, a mixture of proteases and Proteinase K was effective at removing them suggesting these biofilms are largely composed of protein and teichoic acids. DNaseI was also required for eDNA removal in both *ica*-dependent and independent biofilms [22,31,32]. Despite the differences in biofilm extracellular matrix composition, during this phase of growth the biofilms begin to

have tower structures separated by fluid filled channels allowing for nutrient dissemination and waste removal [23].

Dispersal

Dispersal is the last step in the biofilm process and occurs in response to quorum sensing signals supplied by the *agr* locus described above [14,22,32,33]. The *agr* locus has an expression cycle which includes its repression during the initial colonization phase, leading to enhanced adherence due in part to up-regulated production of cell surface adhesions. When the cell density increases, the accumulation of the autoinducing peptide (AIP) accumulates to a threshold level which activates the *agr* system and triggers dispersal [22]. Although the exact mechanism is not understood, agr-mediated dispersal is due, in part, to the up-regulation of protease production [22,32]. Agr-mediated dispersal can be induced in a young biofilm through the addition of AIP to the medium [14], and regardless of the stage of biofilm development, bacterial regrowth occurs in voids left by the detached cells [14]. In addition to *agr*, thermonuclease, a secreted temperature stable nuclease, may also be needed for dispersal, presumably by degrading eDNA [22,25,32]. Interestingly, the *agr* response appears to be limited to surface exposed areas and increases biofilm detachment by up-regulating the AIP effector molecule and repressing the attachment factors [33,34]. Naturally occurring *agr* mutants have been isolated from clinical *S. aureus* biofilms with mutations existing in the histidine kinase and sensor domains [35], and these mutants have a thicker, more dense biofilm than their counterparts, presumably allowing for persistence in infection [23,34]. It is postulated that these mutants may be more adept at forming long-term chronic infections due to their increased expression of surface adhesions and repression of factors leading to detachment [36]. However, these

mutants seem to arise naturally *in vivo* and *in vitro* during the extreme stationary phase of growth and biofilm development; many will even arise in samples taken from clinical settings and then cultured for several days planktonically [34]. Aside from Agr signaling, little is known about other cell signaling and communication mechanisms that occur within *S. aureus* biofilms.

Immune Response

The biofilm lifestyle adds an additional challenge to the immune system of the host, resulting in a six-log decrease in bacterial susceptibility to antimicrobials when planktonic cultures are compared to biofilms [32]. This decrease in susceptibility is a particular concern with *S. aureus,* since a great number of *S. aureus* infections (endocarditis, osteomyelitis, chronic wound infections, and infections of implanted medical devices) are caused by biofilms. The traditional means of interacting with a bacterium through antimicrobial peptides (AMPs), neutrophil phagocytosis and the complement system is difficult with aggregates of cells [37,38,39]. Normally this response works in a complement cascade. The pathogen is labeled to facilitate phagocytic uptake via complement receptors. The phagocytes are attracted to the microbes through the production of chemoattractants, which leads to the direct lysing of most Gram-negative cells through a membrane attack complex, and phagocytosis of other cells such as Gram-positive bacteria [37]. To combat the immune system, pathogenic bacteria are equipped with an arsenal of weapons which allow for interaction during all steps of the immune response. Antimicrobial peptides and the complement system can be disrupted through proteolytic degradation, AMP binding and inactivation through D-alanylation of teichoic acids and metalloproteases [40]. Neutrophils have the ability to make extracellular traps or nets, which are degraded by bacterial extracellular

DNAses [41]. There are also a variety of extracellular proteases which have the ability to cleave antibodies [42]. *S. aureus* in particular has the ability to prevent destruction [43] once engulfed through its production of superoxide dismutases [44], catalase [45,46] and golden carotenoid pigment [5]. In addition to being able to avoid destruction, it has the ability to lyse host leukocytes through pore-forming toxin production [41,47]. Within the biofilm, the ability of the immune system to reach the target and interact specifically with individual microbes is much more limited. There may be limited diffusion within the biofilm by antimicrobial peptides and the complement system, in addition to possible active repulsion by the biofilm of these host defenses [48]. Furthermore, the effect of singular immune cells is decreased on such a large population of cells [23]. Although detailed studies of immune cell interactions with *S. aureus* biofilms have not been reported in the literature, this reduced anti-biofilm efficacy has been seen through the interaction of *Pseudomonas aeruginosa* with macrophage secretory products (MSP) [49]. When *P. aeruginosa* was actually grown in the presence of MSPs their virulence was enhanced in a biofilm mouse model of ascending pyelonephritis [49]. Rather than destroying the biofilm, the immune system appeared to actually aid *P. aeruginosa* in its ability to evade phagocytosis [49]. Furthermore, neutrophils interacting with the *P. aeruginosa* biofilms *in vitro* have been shown to become phagocytically engorged and immobilized. In addition, these neutrophils underwent respiratory bursts but no phagocytosis, leading to an increase in oxygen consumption within the system, yet no increase in soluble H_2O_2 [50]. This decrease in efficiency of the immune cells allows the microbes within the biofilm to

proliferate while the neutrophils remained immobilized with a diminished oxidative burst and thus defense potential [50].

Nitric Oxide Signaling

Nitric oxide (NO) is a free-radical gas, which easily diffuses and is highly reactive, making it an important molecule for both cell signaling and host defense in eukaryotes. It is also produced as part of the denitrification pathway of prokaryotes, when nitrate is sequentially reduced to dinitrogen via nitrite, NO and nitrous oxide. High levels of NO may be toxic to these cells, and is thus commonly reduced to nitrous oxide. In eukaryotes it is well known as an endothelial relaxing factor, cytotoxic agent, and nervous system signaling molecule [51]. This versatile signaling molecule has a variety of targets, including heme/nonheme iron cofactors, iron-sulfur clusters, redox metal sites, lipids, DNA and amines [52]. Methods for modification of proteins include S-nitrosylation, the transfer of a nitric oxide group to cysteine sulfhydryls on proteins which is comparable to phosphorylation of proteins [53], and nitration, a covalent post-translational protein modification derived from the reaction of aromatic amino acids (primarily tyrosine or tryptophan) in proteins with NO or other reactive nitrogen species (RNS) [54].

Nitric Oxide Synthases in Eukaryotes

While the targets of NO are abundant, the sources of NO production are much more limited, with one of the main sources being nitric oxide synthase (NOS) [55]. Although present in eukaryotes, prokaryotes, and archaea, the most widely studied *nos* genes are in mammals [56,57]. There are three types of *nos* in mammals, with two being constitutively expressed and one considered an “inducible” NOS. The constitutively expressed NOS are common in the central nervous system, where,

although not stored in the synaptic vesicles, it acts as a neurotransmitter [58]. The second constitutive NOS was discovered in endothelial cells, where it helps maintain basal vascular tone, and is involved in platelet aggregation. Inducible NOS (iNOS) is specific to the immune response, expressed in both neutrophils and macrophages [52].

The NO produced from these NOS enzymes has a variety of roles. Some of the most common roles for NO is through interactions with heme groups and sulfhydryl groups [59], causing perturbation in certain zinc transcription factors [60], and modifications of various proteins and lipids. One of the specific interactions observed in eukaryotes has been with guanylate cyclase which is activated by NO, causing an increase in cyclic guanosine monophosphate (cGMP) [52,61,62,63]. This interaction is one of the categories of NO signaling specific to the calcium dependent constitutive NOS enzymes, known as “cGMP-dependent signaling”. In these cases, NO interacts with a soluble guanylyl cyclase-heme containing a heterodimeric NO receptor. This receptor converts guanosine triphosphate to guanosine 3’5’-cyclic monophosphate, which can then act on protein kinases, gated channels and phosphodiesterases [52]. The other type of signaling is known as “cGMP-independent signaling” [52]. This type of signaling involves nitrate and nitrite being recycled in blood and tissues to form NO storage pools in the event NOS production is insufficient [52]. S-nitrosylation is also cGMP independent and refers to the reaction of NO or an NO derived species with cysteine residues on target proteins. This reaction regulates a variety of cellular targets from protein kinases, proteolytic enzymes and transcription factors, to proteins involved with energy transduction [52].

Nitric Oxide Signaling in Bacteria

Bacteria also respond to NO, oftentimes encountered in the form of nitrosative stress during host infection. NO inhibits DNA replication by mobilizing the zinc from the DNA binding proteins [60]. To prevent this interaction, there are a variety of NO metallo-regulatory proteins produced by bacteria that sense and respond to elevated NO concentrations. *Escherichia coli* has six known NO sensors, including the non-heme sensors NorR and NsrR which respond to nanomolar ranges of NO and the iron-sulfur proteins SoxR and FNR which respond to both superoxide and NO [60]. Although well studied in *E. coli,* this motif is conserved across many bacteria in a heme NO and/or oxygen binding (H-NOX) domain. Although there are no known "true" zinc sensors of NO in *E. coli,* the *Neisseria gonorrhoeae* NmlR protein is a zinc containing transcriptional regulator which responds to NO and mediates the nitrosative stress response through 5-nitrosoglutathione reductase activity [60]. In *Mycobacterium tuberculosis* the proteins commonly interacting with NO may actually be oxygen sensors, and NO binding prevents oxygen binding which mimics a low oxygen situation, causing histidine kinase activation [52]. In *S. aureus,* the Staphylococcal Respiratory Regulator (SrrAB) and Flavohaemoglobin (Hmp) are the best-studied sensors of NO, with SrrAB involved in regulating the nitrosative stress response and Hmp directly detoxifying the NO [64]. SrrAB is homologous to ResDE in *Bacillus subtilis,* which has also been shown to act as an NO sensor in this organism. ResDE is a two-component system which activates the transcription of genes required for nitrate respiration under oxygen-limiting conditions [65,66], in addition to genes involved in NO detoxification such as the flavohaemoglobin gene *hmp* [66]. Likewise, *S. aureus* SrrAB is also involved in regulating the expression of the *S. aureus hmp* gene [64,67,68,69,70,71].

SrrAB is also involved in the *S. aureus* nitrosative stress response, as a *srrAB* mutant displayed increased sensitivity to NO [64].

The Role of Nitric Oxide in Biofilm

NO has also been shown to play a crucial role in affecting bacterial biofilm formation. One of the few studies looking into the role of NO in *S. aureus* biofilms looked at inhibition of biofilm formation through acidified nitrite repression of the *icaADBC* gene cluster [72]. This interaction with the acidified nitrite appeared to cause a stress response which impaired the biofilm's ability to deal with oxidative and nitrosative stress (as determined by RNA microarray) as well as through decreased PIA production.[72]. In this same study, biofilm growth that was inhibited in the presence of acidified nitrite could be recovered through the addition of an NO scavenger, suggesting that NO was generated as a byproduct of the disproportionation of the unstable acidified nitrite, and was directly or indirectly responsible for the observed phenotypes [72].

In *P. aeruginosa,* exogenous NO has been shown to cause biofilm dispersal, aiding in the complete removal of a biofilm with the addition of an antimicrobial [15,73]. Endogenous NO production, via denitrification [73], also appeared to trigger cell death and dispersal, while an added oxidative or nitrosative stress on *Pseudomonas* biofilm has been shown to cause bacteriophage induction and cell lysis [15,73]. This interaction was c-di-GMP dependent and a decrease in c-di-GMP led to dispersal of the biofilm, while an increase led to increased adherence [74]. This decrease in c-di-GMP is hypothesized to occur when NO stimulated certain phosphodiesterases, causing c-di-GMP breakdown and dispersal.

In *Neisseria gonorrhoeae,* the effect of NO was tested on both early and late phases of biofilm development [74]. During the early phases of biofilm development,

high levels of exogenous NO prevented biofilm formation. However, later in biofilm formation, once anaerobic respiration has been initiated, the addition of low levels of NO actually enhanced biofilm formation, suggesting that NO may perform multiple regulatory roles during the course of biofilm development in this bacterium [74].

Bacterial NOS

From the evidence described above, NO appears to be an important signaling molecule in bacteria, and one of the potential sources of endogenously produced NO is the bacterial *nos* gene, which is mainly confined to Gram-positive pathogens [75]. Bacterial NOS produces NO by catalyzing a five electron oxidation of a terminal guanido nitrogen of L-Arg and takes 2 moles of oxygen and 1.5 moles NADPH per mole of NO produced. This occurs through two reactions: the conversion of L-arginine to N-ω-hydroxy-L-arginine (NOHA) and the conversion of NOHA to citrulline and NO [76,77]. Eukaryotic NOS has both an oxygenase and reductase domain and these reactions occur in a calcium-dependent reaction [51,76,78,79]. The prokaryotic NOS was identified via genomic sequencing, and has homology to the catalytic oxygenase domain of eukaryotic NOS [79,80,81]. This homology includes the heme-binding and active sites of the enzyme with one conserved valine residue in the eukaryotic catalytic domain that is replaced by a conserved isoleucine residue in bacteria [51,82,83]. The notable exception to prokaryotes only having the oxygenase domain is in the NOS of the Gram-negative bacterium *Scrangium cellulosum,* which also has a covalently attached reductase to the N-terminal domain, separated from the oxygenase domain by an area of unknown function [75].

Structurally, bacterial NOS resemble a “catcher’s mitt” fold with a heme group in the center and a winged beta sheet and helix turn motif [84]. There is a hydrophobic

“helical lariat” for a pterin cofactor to bind, and unlike eukaryotes, there is no terminal zinc-binding domain restricting the size of the cofactor [51,80,85]. When unfolded, the NOS dimer interface is highly disordered, and this disarray prevents heme-based oxygen reduction without the proper substrate and cofactor [75,81,84]. This structure, since there is no reductase domain, needs to accept electrons from other sources. These reductases are not as efficient as the single eukaryotic domain, and are often multiflavin-containing sulfite reductases [86]. Even though there is not a specific redox partner identified for bacterial NOS, over-expression of the *nos* gene in a bacterium which does not code for it normally, such as in *E. coli,* can compensate for the lack of a dedicated redox partner through its native enzymes [51,87].

In addition to varying redox partners, the location of *nos* on the chromosome changes from bacterium to bacterium, but the location may not always correlate with the role played by NOS. For example, in *Deinococcus radiodurans* the *nos* gene is not located near its target, the tryptophanyl-tRNA synthetase (TrpRSI) whose interaction is mediated by the NOS-interacting protein (TrpRSII, which has a low level of homology to typical TrpRSs) [88]. TrpRSII increases *nos* affinity for arginine and produces 4-nitro-Trp-tRNA which may be used as a substrate for protein or metabolite biosynthesis [51,89,90,91]. In comparison, *Streptomyces turgidiscabies* has *nos* located five genes upstream from *txtABC*, an operon responsible for thaxtomin production [92]. Thaxtomin is a phytotoxin that causes potato scab disease, and its NOS is responsible for nitration of the thaxtomins on a tryptophan moiety which is important for the functionality of thaxtomins, stimulating the roots of infected plants to grow and increase tissue production, allowing for further colonization by the bacterium [59,92,93]. In *B. subtilis*

and *Bacillus anthracis,* NOS increases antibiotic tolerance through both chemical modification of antibiotics and reducing the cellular oxidative stress that ensues from the actions of many antimicrobials [94]. NOS-derived NO also protects these bacteria from oxidative and nitrosative stress by activating catalase and inhibiting enzymes capable of reducing thiols, thus preventing the formation of hydroxyl radicals and DNA damage [75,95]. Hydrogen peroxide toxicity and thus DNA damage occurs by way of the Fenton reaction, which occurs when hydrogen peroxide interacts with free cellular iron. To drive this reaction, ferric iron must be continuously re-reduced to the ferrous state through cellular reductants such as cysteine. In *Bacillus,* it is postulated that this reaction can be suppressed via endogenous NO by its transient nitrosylation of the cysteine residues of proteins and thus inhibiting cysteine reduction in the cell [96]. The ability to withstand oxidative and nitrosative stress plays a role in virulence, enabling the bacteria to survive when attacked by macrophages and neutrophils. For example, without the *nos* gene, the virulence of *B. anthracis* within a mouse model was greatly reduced and the ability to survive within a macrophage was also reduced [51]. However, a role for *nos* in bacterial biofilm development has not been explored.

Staphylococcus aureus nos

S. aureus is another Gram-positive pathogen which codes for an active NOS enzyme, which can bind large ligands and is most similar to the iNOS of the immune system [51]. It has been crystallized with a nicotinamide ring of NAD bound in the cofactor site, which although not biologically relevant, has shown the structure is homologous to the eukaryotic NOS oxygenase domain and has the dimer formation [97]. This NOS has also been shown in vitro to break down arginine to citrulline with NO as a byproduct [98], and provides one of three postulated routes of endogenous NO

production in *S. aureus* (Figure 1-2). The affinity of NOS for L-arginine is increased by the addition of a tetrahydrobiopterin or one of its analogs, and the enzyme can bind bulky ligands such as nitrosoalkanes and tert-butylisocyanide [99]. The other postulated sources of NO production in *S. aureus* (disproportionation of acidified nitrite, and NO directly produced by a nitrate reductase), could also contribute to NO signaling within *S. aureus* (Figure 1-2), but due to its unique association with pathogenic bacteria, it is possible there is a more specific role for SaNOS. In *S. aureus,* NOS was shown to act as a means for dealing with hydrogen peroxide stress under planktonic conditions [94]. In addition, a *nos* deficient strain of *S. aureus* RN4220 was reported to be more susceptible to antibiotics such as cefuroxime, acriflavine and pyocyanin [94]. This *nos* mutant has also been reported to have increased sensitivity to oxidative stress, similar to *B. subtilis* [96]. Given that these data were generated in a chemically mutated *S. aureus* lab strain that is known to contain several mutations [132], it is important to further investigate a role for the *S. aureus nos* gene during planktonic growth, and biofilm development in a clinical isolate, such as UAMS-1. Therefore, the purpose of this study is twofold: (1) To characterize the phenotype of a *S. aureus* UAMS-1 *nos* mutant under both planktonic and biofilm conditions and (2) To determine the expression pattern of the *nos* gene under these same conditions. Based on the described effect of NO on biofilms in other bacteria, we hypothesize that SaNOS contributes to *S. aureus* biofilm development, possibly by production of NO as a cell-signaling molecule.

Table 1-1. Examples of virulence factors responsible for *Staphylococcus aureus* pathogenicity.

Virulence Factor	Role in Virulence	Example	Source
Secreted Toxins			
Cytolytic	Form pores in host cell cytoplasmic membranes, cause lysis	Hemolysins, leukocidins, PSM, α toxin, PVL	[100,101]
Superantigen	Immune-stimulatory, cause capillary leak, epithelial damage, hypotension	Enterotoxins A, B, C, D, E, G, Q, TSST-1	[100,102]
Exoenzymes			
Beta Lactamase	Inactivates penicillin, works with penicillin binding proteins	Penicillin binding protein	[1,100]
Protease	Actively degrade human protease inhibitors, tissue degradation Degrade host macromolecules i.e. collagen, elastin, fibronection	Serine (SspA), cysteine (SspB)	[100] [103]
Lipase	Scavenge host sterols for bacterial membranes	Sal-1, sal-2	[104]
Coagulase	Prothrombin activator, Role in virulence unclear	Coagulase (coa)	[100]
Self Surface Adhesions			
MSCRAMMS	Mediate microbial adhesion to host factors: fibronectin, collagen, fibrinogen, immunoglobulin, integrins	fnbpA, fnbpB, CAN, CLF, Protein A, filamentous hemagglutinin	[26,100]

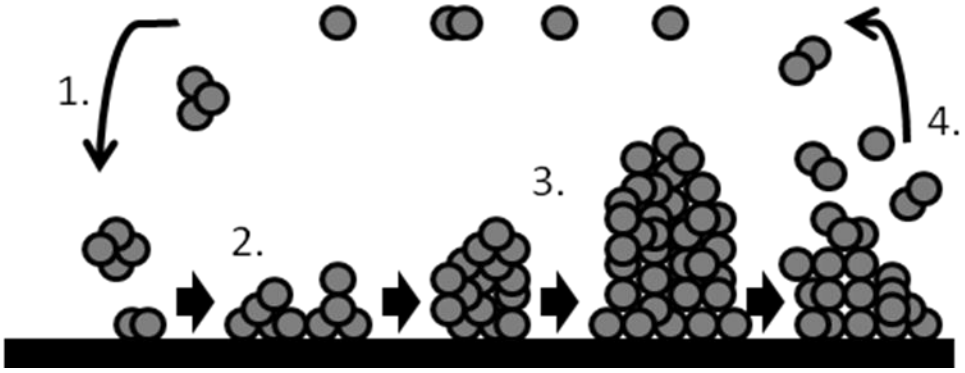

Figure 1-1. Biofilm development in *S. aureus.* 1. Cells leave the planktonic state and attach to a surface to become part of a sessile community. 2. An extracellular matrix is formed and more cells aggregate to the area. 3. Maturation occurs where the biofilm grows in biomass and structures may form. 4. Microcolonies of cells disperse to colonize new areas.

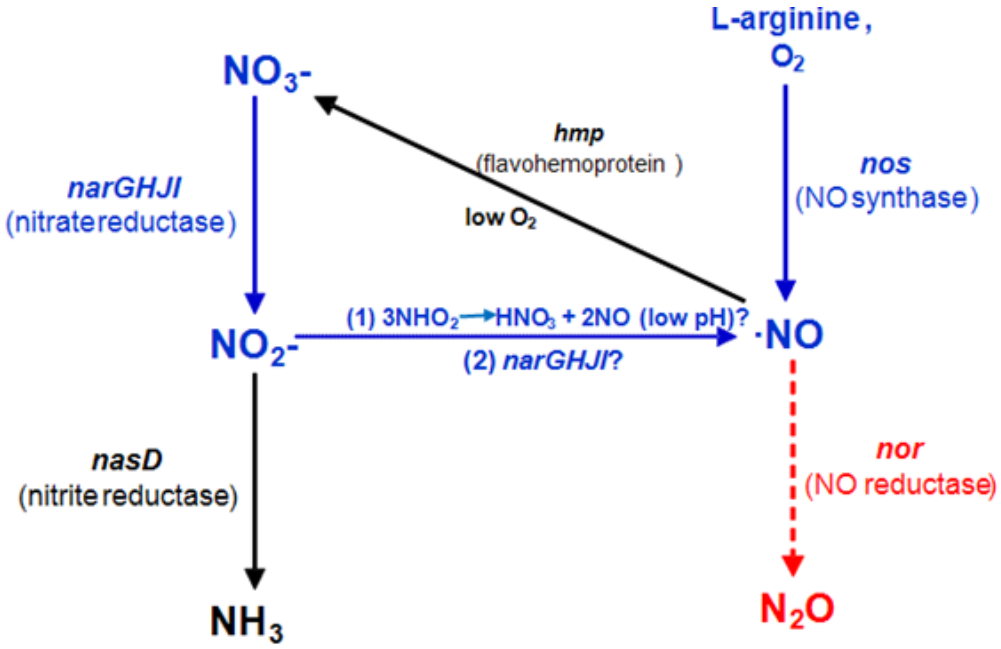

Figure 1-2. Postulated routes for NO formation and consumption in *S. aureus.* The potential routes for NO metabolism depicted above are based on the presence of these genes in the *S. aureus* MRSA252 sequenced genome (a closely-related strain to UAMS-1) [105], in combination with published data from *S. aureus* and/or other NO-producing bacteria. The potential routes of endogenous NO production are depicted in blue. The gene depicted in red is not conserved throughout all published *S. aureus* genomes, however it is present in the UAMS-1strain used in this study, in addition to the published genome of MRSA252.

CHAPTER 2
MATERIALS AND METHODS

Bacterial Strains and Growth Conditions

The *Staphylococcus aureus* strains used for this study are listed along with plasmids used in Table 2-1. All planktonic *S. aureus* cultures were grown either aerobically (1:10 volume to flask ratio, 250 RPM) or under low-oxygen conditions (7:10 volume to flask ratio, 0 RPM), in tryptic soy broth (TSB) or in biofilm medium (TSB-NaGlc: TSB supplemented with 3% (wt/vol) NaCl and 0.5% (wt/vol) glucose). Where indicated, antibiotics were used at the following concentrations: 5 µg/mL or 10 µg/mL chloramphenicol (Cm), 2 µg/mL or 10 µg/mL erythromycin (Erm). *E. coli* was grown under the same aerobic conditions in Luria-Bertani (LB) broth with 50 µg/mL ampicillin (Amp) or 50 µg/mL Kanamycin (Km). Glycerol stock cultures were maintained at -80ºC and were prepared by mixing equal volume of overnight culture with sterile 50% (vol/vol) glycerol in cryogenic tubes. For each experiment described below, a fresh *S. aureus* culture of each strain was streaked from its frozen stock onto tryptic soy agar (TSA) containing the appropriate selective antibiotic as indicated in Table 2-1.

Creation of *nos* Mutant and Complement Strains

Plasmid pTR27 and the *nos* mutation in strains Newman and COL were created by Dr. Anthony Richardson (University of North Carolina at Chapel Hill), whereas the *nos* mutant in strain UAMS-1 was created using pTR27 by Dr. Kelly Rice (University of Florida). In brief, plasmid pTR27 was created as follows: The *nos* gene was amplified from strain COL by PCR using the primers specified in Table 2-2 and “Topo-cloned” into pCR2.1 (Invitrogen) to generate pTR10. An internal *Bgl*II site was introduced in this cloned sequence 232 bp downstream from the NOS start codon in the sequence 5'-

gttaaatgtcattgatgcaagAGATGTtactgacgaagcatcgttcttatc-3', where the capital letters are located, changing the sequence from AGATGT to AGATCT, a *Bgl*II restriction enzyme cut site. An *Eco*RI fragment harboring this modified allele was moved into the *Eco*RI site of pBluescript SK to generate pTR11 making the engineered *Bgl*II site unique. A 1.1 kb *Bam*HI-digested fragment harboring an erythromycin (Erm^R) cassette from Tn1545 [106] was then cloned into the unique *Bgl*II site of pTR11 to generate pTR12 (*nos*::Erm^R in pBluescript SK). The *Eco*RI fragment of pTR12 carrying the *nos::*Erm^R allele was ligated into *Eco*RI in the temperature sensitive shuttle vector pBT2 to generate pTR27.

To create *S. aureus nos* mutants with pTR27, this plasmid was first transformed into strain RN4220 (a chemically-mutated *S. aureus* strain that more readily accepts foreign DNA) by electroporation, then phage-transduced into strains Newman, COL and UAMS-1 using standard methods, with growth at 30ºC [107,108,109]. Integration of pTR27 into the *nos* gene on the *S. aureus* chromosome was achieved as follows: *S. aureus* COL, Newman or UAMS-1 harboring plasmid pTR27 was grown at 43º C in the presence of erythromycin (non-permissive temperature for plasmid replication), to promote integration of the plasmid into the chromosome via homologous recombination at the *nos* gene. To induce a second recombination event, a single isolated colony was then used to inoculate TSB (no antibiotic) and grown at 30°C for 5 days. Every 24 hours, an aliquot of the culture was diluted 1000-fold into fresh TSB (no antibiotic). On days 3-5, the culture was serially-diluted and spread on TSA plates containing erythromycin, and isolated colonies were then screened for erythromycin-resistant and chloramphenicol-sensitive phenotypes by picking and patching onto TSA-Erm^2 and

TSA-Cm^5 plates. PCR (with the same primers used to clone the *nos* gene in pTR27) and Southern blotting were both used on candidate mutants and appropriate control strains to confirm that the chromosomal *nos* gene had been correctly replaced by the *nos*::Erm allele (data not shown).

In this study, the stability of the *nos::*Erm mutation in UAMS-1 was confirmed by streaking the mutant out on TSA+Erm^2 medium and then overnight culturing representative colonies in TSB without antibiotic. Serial dilutions were made on these overnight cultures and the 10^{-7}-10^{-9} dilution range was plated on both TSA plain and TSA+Erm^2. The colonies were then counted to ensure comparable CFU/mL on each plate, to confirm the mutation is stable. With $8.3x10^8$ colonies on the TSA+Erm^2 plates and $7.5x10^8$ colonies on the TSA plain plates (average of three replicates), the mutation was determined to be stable.

The *nos* mutation in UAMS-1 was complemented in this study using a "gene knock in" strategy, whereby the appropriate primers specified in Table 2-2 and Thermalace enzyme (Invitrogen) were used to PCR-amplify a 2.5-kb genomic fragment from UAMS-1. This PCR product encompassed 750-bp upstream (nucleotide 2,098,174 of the MRSA252 genome, Genbank accession # BX571856) of *nos* (annotated as SAR2007 in the MRSA252 genome) and 615-bp downstream of *SAR2008* (nucleotide 2,101,429 of the MRSA252 genome) (Figure 2-1). The PCR product was gel purified using a ZymoResearch gel purification kit and then cut with *EcoR*Vand *Pst*I (naturally-occurring restriction sites upstream of *nos* and downstream of SAR2008, respectively) and ligated to pBT2, which was also gel purified and cut with the same enzymes. The ligated plasmid was transformed into *E. coli* by heat-shock [110] and confirmed by

isolating plasmid from potential clones using the Promega Wizard Miniprep kit, followed by restriction-enzyme digestion with *EcoR*V/*Pst*I and agarose-gel electrophoresis to visualize the reactions. Following confirmation, the plasmid was electroporated into RN4220 [109] and spread on Cm^{10} plates and grown at 30ºC, the permissive temperature for replication of pBT2. The resulting colonies were then cultured overnight in TSB-Cm^5 and plasmid DNA purified from these cultures was screened as described above, to confirm the correct insert size. Following confirmation, the plasmid was transduced into KR1010, the UAMS-1 *nos::*Erm mutant [108]. A transductant that was confirmed (as described above) to have the plasmid was then grown on TSA-Cm^{10} at 43ºC (non-permissive temperature for plasmid replication) in the presence of chloramphenicol to select for cells which had integrated the plasmid into the chromosome. In order to promote a second recombination event, a single colony was grown at 30ºC for five days, and each day the culture was diluted 1:1000 into fresh TSB. After the third, fourth and fifth days the culture was diluted and plated on plain TSA, and individual colonies were selected and screened for sensitivity to both erythromycin and chloramphenicol. Verification that the potential complement strains were correct was carried out via Southern blot analysis [111] and PCR amplification (data not shown). The complement strain was designated KR1011.

Bioscreen C Planktonic Growth Assays

The Growth Curves USA Bioscreen C was used to compare planktonic growth of the wild-type UAMS-1, *nos::*Erm mutant and complement strains. For each replicate, a single colony from a freshly-streaked plate was used to inoculate 3 mL TSB and grown at 37ºC and 250 rpm for 24 hours. The OD_{600} of each overnight culture was recorded and used to inoculate 0.50mL of TSB (or TSB-NaGlc, depending on the experiment) to

an OD_{600}=0.05. 250µL of each diluted culture was added per well of the Growth Curves USA 100 well Bioscreen C plate, in duplicate for each replicate. The Bioscreen C was run on fast, continuous shaking for 72 hours at 37ºC, and OD_{600} measurements were recorded every 45 minutes. For the wells treated with hydrogen peroxide (H_2O_2), the initial inoculum was supplemented with 20mM (final concentration) H_2O_2 and grown under the same settings described above. Each growth curve was performed on at least n=5 biological replicates of each strain.

Qualitative and Quantitative Pigment Assays

The pigment differences in the wild-type UAMS-1, Newman and COL strains compared to their respective *nos* mutants was qualitatively assessed by growth on TSA in the absence of antibiotic selection. Each strain was initially streaked out on TSA (with selective antibiotic as necessary), and then a single colony from each was used to inoculate 3 ml TSB (no antibiotic) and incubated overnight under aerobic growth conditions. The OD_{600} of each culture was taken the next day and each culture was diluted in 1mL of TSB to an OD_{600} =0.50. The cultures were then plated in 10 µL drops on TSA plates (no antibiotic) and left to grow at 37ºC for two days, to promote maximal pigment production [5]. Plates were then photographed with a digital camera. This experiment was repeated on 3 biological replicates of each strain.

Pigment production in UAMS-1, KR1010 and KR1011 was also quantified from planktonic TSB cultures (initially inoculated to OD_{600}=0.05) that were grown for 24 and 48 hrs at 37ºC and 250 RPM, as well as from cells scraped off from TSA plates grown for 24 and 48 hours at 37ºC. Each condition was assayed in biological triplicate. The methanol extraction method from Morikawa et al. [112] was used, to isolate the pigment. 800uL of each overnight culture was diluted to an OD=3.0, spun down and washed with

water before being treated with methanol at 55ºC for 5 minutes. The extracts were spun down again and the supernatants were brought up to a volume of 1 mL and compared against a methanol standard. Absorbance was read at 465nm, the maximum absorption wavelength for carotenoids. Statistics were performed using a one way analysis of variance and the Student-Newman-Keuls method.

Biofilm Assays

To determine phenotypic differences between UAMS-1, KR1010 and KR1011 with regards to biofilm development, static biofilm assays were performed in triplicate. A Thermo Scientific Nunc 8-chamber glass slide was pre-coated for 24 hours at 4º C with 350µL 20% (vol/vol) human plasma (Sigma) in bicarbonate buffer (Sigma Carbonate-Bicarbonate capsules, 1 capsule dissolved per 100mL of water). After coating, the plasma was removed and wells were each inoculated with 500µL fresh overnight *S. aureus* culture grown in TSB-NaGlc (described above) and diluted to OD_{600} =0.05 in the same TSB-NaGlc biofilm medium. Static biofilms were grown for 24 hours at 37 ºC, culture supernatants were removed and biofilms were stained with LIVE/DEAD stain (Invitrogen) using 1.5 µL/mL propidium iodide (PI) and 0.5µL/mL Syto 9 prepared in 0.85% (vol/vol) NaCl. Staining occurred for 30 min at room temperature, covered with aluminum-foil to preserve light sensitivity. The stain was then removed and 500 µL 0.85% NaCl was added to each of the wells prior to imaging by confocal microscopy. The images were acquired on a Zeiss Pascal LSM5 Confocal Laser Scanning Axiovert 200 Microscope using an Argon-laser and a 40x water immersion lens. For each biological replicate, six representative images were taken of each well, for a total of 18 z-stacks acquired per strain. The z-stacks were taken at 0.5 µm z-slice intervals and a scanning speed of 8, on frame mode. The images were processed using the LSM

Browser software (Zeiss) and biofilm characteristics were quantified using COMSTAT software for MatLab [113].

RNA Isolation

The RNeasy micro RNA isolation kit (Qiagen) in combination with the FASTPREP-24 and lysing matrix B (MP Biomedicals LLC) were used to obtain RNA from UAMS-1, KR1010 and KR1011 under aerated and low oxygen growth conditions in triplicate, by previously described methods [114,115]. The “aerated RNA” was harvested from cells at t=6 hours only whereas the “low oxygen RNA” was obtained at both t=2 and t=6 hours growth (corresponding to early-exponential and late-exponential growth phase, respectively). 25mL of each culture was spun down (4,500 rpm) in 50mL falcon tubes for each RNA isolation, and at the t=6 time point under aerobic and low oxygen growth, the final elution was done twice for a final volume of 100µL. Following RNA isolation, Northern blotting was performed with the DIG system (Roche) (probe primers are listed in Table 2-2) according to manufacturer’s protocols and previously published methods [115].

RNA was also obtained after cultures were treated with H_2O_2. In brief, UAMS-1, KR1010 and KR1011 were cultured in TSB. The cultures were grown for 11 hours, and a 1:1000 dilution was made into fresh TSB. The cultures were grown until the OD_{600}=0.80 then a 1:100 dilution was made into fresh TSB. When the culture reached an OD_{600}=0.80 again, the cultures were treated for 20 minutes with 10mM H_2O_2. Following treatment, RNA was obtained as described above. This experimental design was adapted from Chang et al. [116], who by RNA microarray had shown an up-regulation of *nos* expression 20 minutes after exposure to 10mM H_2O_2. This experiment was only performed once for each strain.

cDNA Production and Quantitative Real-Time PCR (qRT-PCR)

The iScript cDNA synthesis kit from BioRad was used to make a cDNA pool generated with random primers as described in the manufacturers protocols from the RNA isolations described above. In brief, each RNA sample was quantified using a Nanovue (General Electric) on the default RNA settings and then 0.750µg RNA was added to each cDNA reaction. This cDNA was then used in qRT-PCR to quantify the amount of *nos* and bifunctional purine biosynthesis protein (*purH*) (using primers listed in Table 2-2) in the 2 and 6 hour low oxygen samples, and in the 6 hour aerobic samples, using the iQ SYBR green supermix (Biorad) detection method. Transcription of *nos* was also assessed by this method in the RNA samples isolated from the H_2O_2-treated cultures. The qRT-PCR took place in a BioRad iQ5 thermal cycler. The protocol was one cycle at 95ºC for 3 minutes, followed by forty repeats at 95ºC for 15 seconds and 55ºC for thirty seconds. This is then followed by 81 repeats of 30 seconds of increasing the temperature from 55ºC-95ºC with the set point temperature increasing after cycle 2 by 0.5ºC to generate the melting curve. The genes of interest were compared against a standard, in this instance the σ^{70} gene, which is the housekeeping sigma factor in *S. aureus*. Due to its nature as a housekeeping gene, it should have stable transcription despite the growth phase, and thus provide an accurate standard to account for loading differences and varying PCR efficiencies [117,118]. A suitable reference gene should have a standard deviation of less than 2-fold from the mean expression level of the given gene, a criterion which is satisfied by σ^{70} [119]. The Livak ($\Delta\Delta C_T$) method was used to determine relative fold change (see sample calculations in Appendix 1). This method was used because the amplification efficiency for each set of primers was near 100% and each primer set amplified within 5% of each other [120].

Co-Transcription PCR

To determine whether the *nos* and *SAR2008* genes are co-transcribed, a primer pair was designed to amplify the intergenic region between these two genes (see Figure 2-1). Specifically, these primers were located 718 bp upstream from the *nos* stop codon and 162bp downstream from the SAR2008 start codon. This region is 127bp downstream from the Erm cassette insertion in the *nos* mutant. A PCR reaction was run using 75ng of isolated UAMS-1, KR1010, KR1011 genomic DNA, RNA and cDNA (generated with the superscript cDNA synthesis kit described above). The PCR reaction took place in a MJ Mini Personal Thermal Cycler (BioRad), and the reaction conditions were 94ºC for two minutes followed by 20 cycles of 94º for 30 seconds, 50º for 30 seconds then 72º for 2 minutes. After the 20th cycle, there was an additional 72ºC incubation for 10 minutes. A sample of 20µL PCR product with 2µL 6x loading dye was then loaded for each reaction and electrophoresed through a 1% agarose gel at 120V for 45min. The gel was imaged on Molecular Imager Gel Doc XR+ and used with Quantity One software. This experiment was performed twice to ensure reproducibility of the results.

GFP Assays

GFP reporter plasmids were made using the primers described in Table 2-2 and UAMS-1 DNA was used as template, and Thermalace (high-fidelity) enzyme (Invitrogen). The Reaction ran for 94ºC for two minutes, followed by 30 cycles of 94ºC for 30 seconds, 50º for 30 seconds then 72º for 2 minutes. At the end of the cycles there was an additional elongation step at 72º for ten minutes. The primers amplified a putative promoter region 500bp upstream from the *nos* start codon (Figure 2-1). The promoter fragment was initially ligated into pCRBlunt (Invitrogen) and transformed into

E. coli. After confirmation, this plasmid was digested with *Sph*I and *Bam*HI (sites engineered in the forward and reverse primers, respectively), and the resulting fragment was gel purified using a Zymoclean Gel DNA Recovery Kit and ligated into pJB36, which was cut with the same enzymes and gel-purified. This ligation was transformed into *E. coli* DH5α cells via heat shock, with the resulting plasmid designated as pJB-nos, whereby the 500-bp *nos* promoter fragment was cloned upstream to GFP (originally amplified from plasmid pBURSA [121] and containing a 28-bp translation enhancer region [122]. A promoterless GFP plasmid was also made by taking *SphI/Bam*HI digested pJB36, performing a "Klenow" treatment (New England Biolabs) as described by the manufacturer, religating and transforming the plasmid into *E. coli* DH5α by heat shock. This promoterless GFP plasmid was designated pJB36Δ. Each plasmid was then electroporated into *S. aureus* RN4220 [109] and subsequently transduced into UAMS-1 [108].

After confirmation of the plasmids, fluorescence analysis was done to compare promoter activity of pJB-nos, pJB-cidA (a positive control for fluorescence, previously created by Dr. Rice using the cloning strategy described above), and pJB36Δ (a promoterless GFP vector to serve as a negative control for background fluorescence) in UAMS-1 under planktonic growth conditions. UAMS-1 harboring each of these constructs was grown aerobically and under low oxygen conditions in TSB as described above. Each culture was inoculated with a corresponding overnight culture to an OD_{600}=0.1. The cultures were monitored for fluorescence at 2, 4, 6, and 8 hours post-inoculation, whereby samples of each culture were centrifuged and resuspended in 1 mL of 0.85% NaCl. This experiment was performed in biological duplicate.

The fluorescence of each of these constructs was also measured when strains were each grown on TSA plates (in triplicate) under the following environmental conditions: (1) aerobic ("normal" atmospheric conditions) at 37 º C, (2) in a microaerobic (O_2 concentration 6-12%, CO_2 concentration 5-8%) pouch (Remel) at 37 ºC and (3) in a 5% CO_2 incubator at 37 ºC. The cultures (UAMS-1 containing either pJB36-nos or pJB36Δ) were each initially streaked out on TSA-Erm from frozen stocks and then re-streaked onto TSA plain. These cultures were grown for 24 hours under their respective condition, and then the cells were scraped off the agar surface and resuspended in 1 mL of 0.85% NaCl.

For all of the fluorescence experiments, a Biotek Synergy HT plate reader was used to take readings from a 96-well plate (Costar, black with clear bottom) loaded with 200µL of each sample per well, in duplicate. The plate reader was set to read fluorescence from the bottom of the plate. The readings were taken using the Gen5 version 1.09 which took a RFU reading with filter settings of 485/20 excitation and 516/20 emission and sensitivity of 75 for the plate experiments and 65 for planktonic culture studies. Although the density of cells in each well were similar, a corresponding OD_{600} reading was also taken for each well, to calculate the RFU/OD_{600} which would account for slight variations in OD.

Table 2-1. Strains and plasmids used in this study.

Strain or plasmid	Description	Reference
Escherichia coli		
DH5α	Host strain for construction of recombinant plasmids	[123]
Staphylococcus aureus		
RN4220	Easily transformable restriction deficient strain	[124]
UAMS-1	Osteomyelitis clinical isolate	[125]
KR1010	UAMS-1 *nos*:: Erm insertion mutant	This work
KR1011	KR1010 complement strain	This work
Newman	Lab Strain	[126]
AR0100	Newman *nos::*Erm	Obtained from A. Richardson, UNC Chapel Hill
COL	MRSA Lab strain	[127]
AR0093	COL *nos::*Erm	Obtained from A. Richardson, UNC Chapel Hill
Plasmids		
pTR27	*nos::*Erm mutant allele Erm^R/Cm^R	Obtained from A. Richardson, UNC Chapel Hill [128]
pJB36	pCN51; P_{CAD} promoter-GFP; Erm^R	Obtained from K. Bayles, UNMC
pJB36-cidA	*cidA* promoter-GFP Erm^R	Obtained from K. Bayles, UNMC
pCRBlunt	Zero Blunt PCR Cloning kit; Km^R	Invitrogen
pJB36-nos	500bp *nos* promoter-GFP Erm^R	This work
pJB36Δ	promoterless-GFP Amp^R/Erm^R	This work
pBT2	*E. coli-S. aureus* shuttle vector with thermosensitive origin of replication for *S. aureus* Cm^R	[129]
pBT2nos	*nos* complement Cm^R	This work

Table 2-2 Primers and probes used in this study.

Primer Role	Forward/Reverse	Oligonucleotide sequence (5'-3')
nos insertion mutant	Forward	GTTAGTTACCAAAGCATAATTGCG
	Reverse	ATCTGCCACAATGTTGATTGTTCC
nosSAR2008 knock in	Forward	CCCGCATGCATACCAAATAATTTACCCGCCCTA
	Reverse	CCCGGATCCTTGAACGAGTGGTAACGAA
nos qRT-PCR	Forward	TATGGTGCTAAAATGGCTTG
	Reverse	ACGATGCTTCGTCAGTAACA
σ^{70} qRT-PCR	Forward	CAAGCAATCACTCGTGCAAT
	Reverse	GGTGCTGGATCTCGACCTAA
purH qRT-PCR	Forward	CGAAATAAACCGCAGCATTT
	Reverse	TCGTCACATCAGGGTTAGCA
nosSAR2008 co-transcription	Forward	TGGACCTAAAATTTTCAACAA
	Reverse	TGCAACTGACTTGATGACTT
nos promoter region	Forward	CCCGGATCCTAACAATGGTTCGTTACCAAAG
	Reverse	CCCGGATCCACTCTTAAAAATTATGTATATGTCA
nos Northern probe	Forward	AGCAAATCACTTCGGTTGGA
	Reverse	ATTCAACAAGTGCTCGATCT
SAR2008 Northern probe	Forward	GTTCGAACACCATTTCTGAT
	Reverse	CCTGAACGAAAAATCGATAC

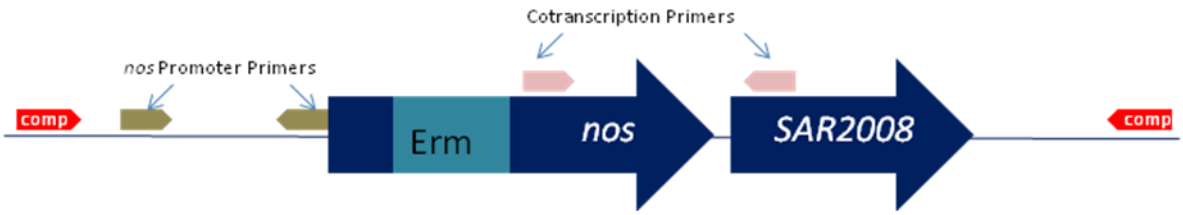

Figure 2-1. Diagram representing primer locations for *nos* complementation (red), *nos-SAR2008* co-transcription (pink), *nos* promoter (brown). The location of the erythromycin cassette is also indicated in the construction of *nos*::Erm.

CHAPTER 3
RESULTS

nos and SAR2008 Are Co-transcribed

During the construction of the UAMS-1 *nos* mutant and complement strains, a closer inspection of the *nos* genomic region revealed that the *nos* gene and the downstream SAR2008 open reading frame, encoding a putative prephenate dehydratase, are only separated by 20 bp, suggesting that *nos* and SAR2008 may be co-transcribed as an operon. To investigate this further, PCR amplification with primers designed to amplify the intergenic region between *nos* and SAR2008 (see Table 2-2 and Figure 2-1) was performed on genomic DNA isolated from UAMS-1, KR1010 (*nos::*Erm) and KR1011 (complement strain), in addition to cDNA and RNA isolated from these strains. As demonstrated in Figure 3-1, genomic DNA amplification yielded the same PCR product in all three strains. This was expected, since the forward primer is positioned downstream from the Erythromycin cassette inserted in the *nos* mutant strain (KR1010). In contrast, cDNA amplification with these same primers occurred in UAMS-1 and KR1011 (a slight decrease in KR1011 may be due to inefficiency during cDNA generation or PCR amplification), but this amplicon was not detected in the cDNA from KR1010. The lack of this PCR product indicates there may be a polar effect on expression of SAR2008 in the *nos::*Erm mutant strain, due to the presence of a terminator hairpin at the end of the Erythromycin cassette. Using RNA template in this PCR reaction did not yield amplification in any of the strains, indicating there was no significant genomic DNA contamination of the RNA samples (Figure 3-1).

Furthermore, Northern blot analysis using *nos* and SAR2008 probes showed co-hybridization present in the wild-type UAMS-1 and neither probe was detected in the

nos mutant KR1010 (data not shown). Therefore, it is important to keep in mind that the phenotypic results described below may be a function of inactivation of the *nos* gene alone and/or due to its polar effect on SAR2008.

Analysis of Planktonic Growth

To determine whether the *nos* mutation affects the planktonic growth of *S. aureus* UAMS-1, the wild-type, *nos::*Erm mutant (KR1010) and complement strain (KR1011) were compared when grown in a Bioscreen C system. As seen in Figure 3-2 and Figure 3-3, when grown in parallel in either TSB or TSB-NaGlc (biofilm media), no appreciable differences in growth of the wild-type, mutant and complement strains were observed by OD_{600} measurements under these conditions. Previous work done by Gusarov and Nudler [96] suggested that endogenous NO production enables bacteria to tolerate oxidative stress, and that NOS-derived NO helped *B. subtilis* and *S. aureus* become less susceptible to reactive oxygen species such as hydrogen peroxide [94,96]. To confirm these results hold true in a clinical isolate, *S. aureus* strains UAMS-1, KR1010 and KR1011 were grown in the presence of 20 mM hydrogen peroxide and growth was measured over a 72 hr period (Figure 3-2). In the presence of hydrogen peroxide, the wild-type and complement strains initially displayed delayed growth but by 24 hours the ODs of the treated cultures of these two strains were close to their respective control (untreated) cultures. In contrast, *nos* mutant strain, KR1010, did not grow in the H_2O_2 medium (Figure 3-2). This observation demonstrates that even though the current *nos* mutant was created in a clinical *S. aureus* strain compared to the previously published studies mentioned above [94,96], the UAMS-1 *nos* mutant also displays increased sensitivity to oxidative stress (H_2O_2) under planktonic growth

conditions. This reinforces the idea that SaNOS plays a role in oxidative stress response in *S. aureus.*

Expression of *nos* under Planktonic Growth Conditions

Interestingly, whole transcriptome analysis done by Chang et al [116] revealed an increase in *S. aureus nos* transcription when cultures were treated with H_2O_2 for 20 min prior to isolating RNA. To determine whether this result holds true in the clinical isolate UAMS-1, a similar experiment was performed. qRT-PCR was used to measure *nos* expression in UAMS-1, KR1010 (no detectable transcription was observed since it is the *nos* mutant), and KR1011 after addition of 10mM H_2O_2 to planktonic cultures. There was a 2.8 fold increase in *nos* transcription when UAMS-1 cultures were treated with H_2O_2 (Figure 3-4B). This result is in agreement with the previously-published microarray results [124]. The growth data presented in Figure 3-2 and the increase in mRNA concentration support a positive role for *S. aureus nos* in responding to oxidative stress.

To obtain a better appreciation for the expression patterns of *nos* under planktonic growth conditions, *nos* expression was also assessed by qRT-PCR on RNA isolated from both aerobically-grown cultures as well as cultures grown under static, low-oxygen conditions. This analysis demonstrated in the wild-type UAMS-1 strain *nos* expression was growth-phase dependent, increasing 6-fold under low oxygen conditions at 6 hours (late exponential phase) relative to 2 hours growth (Figure 3-4). Furthermore, expression of *nos* was up-regulated under low oxygen growth conditions relative to aerobic growth after 6 hours growth. As expected, there was no detectable *nos* expression in the *nos* mutant, and *nos* expression levels in the complement strain were comparable to wild-type levels (Figure 3-4). These results suggest that in addition to being inducible by H_2O_2, the *nos* gene is also expressed under “normal” planktonic

growth conditions in a growth-phase dependent manner, and expression appears to be up-regulated during low oxygen growth

Increased Pigment Production in *nos* Mutant

One mechanism that *S. aureus* uses to combat oxidative stress is through carotenoid pigment production which confers protective antioxidant activity [5]. Qualitatively, the KR1010 (*nos* mutant) displayed consistently increased pigment production relative to wild-type strain when cultured on TSA plates. To follow-up on this observation, pigment production in three different *S. aureus* wild-type strains (UAMS-1, Newman and COL), were compared “side-by-side” with their respective *nos::*Erm mutants after being incubated for two days on TSA plates (Figure 3-5). Qualitative differences in pigment production were not noticeable after 24 hours of growth (data not shown), but at 48 hours, pigment production was consistently higher in all three *nos* mutants relative to their wild-type strains (Figure 3-5). Interestingly, pigment production appeared to be most dramatically increased in strain COL, a lab MRSA strain, and a similar observation was noted when comparing a clinical community-acquired MRSA strain to its isogenic *nos::*Erm mutant (data not shown). To better quantify pigment production in the UAMS-1 background, methanol extraction [112] was used to monitor pigment production at 24 and 48 hours in planktonic TSB cultures, as well as on TSA plates. There was no appreciable difference between UAMS-1 and the *nos* mutant at 24 hours growth under either condition. However, after two days of planktonic growth, there was about a two-fold increase in pigment production in the *nos* mutant compared to wild-type while the complement pigment level was comparable to that of the wild-type. After two days of TSA plate growth, there was about a three-fold increase in pigment in the *nos* mutant compared to either the wild-type or the complement strains (Figure 3-6)

These results were statistically significant as determined by the Student-Newman-Keuls test, where the p-value <0.05.

Interestingly, recent findings published by Lan et al [130] identified hyper-pigmentation mutants in *S. aureus,* with one of these mutants being in the purine biosynthesis gene *purH.* They performed an RNA microarray analysis and found that in the *purH* mutant, there is about 5-fold less expression of *nos* [130]. These results correlate with the observations in this thesis study, as there was increased pigment production in the *nos* mutant, which also has decreased *nos* expression. Therefore, qRT-PCR was also performed on the RNA samples described in the previous section to detect *purH* transcription to see if the reverse relationship (decreased *nos*= decreased *purH* expression) holds true. The results in Figure 3-7 indeed indicated that there is decreased *purH* expression in the *nos* mutant at 6 hours growth in both low-oxygen and aerated growth conditions, and *purH* expression in the complement strain mimicked wild-type levels. At 2-hours growth under low-oxygen conditions, *purH* expression was low in all three strains, which had similar expression levels (Figure 3-7).

nos **Expression under Static Plate Conditions**

As described above, the *nos* mutant displays increased pigment production when grown on TSA plates. Given that decreased *nos* expression appears to correlate with increased pigment production on TSA plates, it was hypothesized that increased *nos* expression may occur in *S. aureus* UAMS-1 under these growth conditions. To test this hypothesis, a *nos* promoter-GFP plasmid reporter construct and a promoter-less-GFP construct (to serve as a negative control for background fluorescence) were each moved into the wild-type UAMS-1 strain, and GFP fluorescence was measured in cells grown under planktonic (aerobic and low oxygen) and TSA medium (aerobic, 5% CO_2

and microaerobic) growth conditions. The promoter activity of *cidA* (a gene studied and known in our lab to be highly-expressed under low oxygen conditions) was also monitored as a positive control for fluorescence and was highly active under low oxygen conditions, suggesting any fluorescence differences observed are not due to insufficient oxygen for proper GFP folding (data not shown). Using this method to monitor *nos* promoter activity, it was observed that a low-level of fluorescence (1500-RFU above background levels under aerobic conditions, 1000-RFU above background levels under low-oxygen conditions) was observed under both planktonic growth conditions (data not shown). These results suggest that *nos* is only expressed at basal levels, or alternatively, only in a “subpopulation” of cells, under these conditions. In contrast, growth of UAMS-1 with the *nos*-GFP reporter plasmid on a TSA plate showed a dramatic increase in fluorescence under normal atmospheric (“aerobic”) conditions (Figure 3-8), as compared to micro-aerobic and 5% carbon-dioxide growth. This decrease in *nos* expression on the micro-aerobic TSA culture relative to the aerobic” TSA culture is in contrast to the planktonic growth *nos* expression patterns observed by qRT-PCR (Figure 3-4), where the low oxygen growth showed an increase in transcription. These differences may indicate a different environmental stress and/or signaling condition triggering *nos* expression under the agar medium growth condition. Alternatively, growth as a “static colony” of bacteria at an air-solid interface may potentially link *nos* to a role in a more sessile community, like a biofilm. Fluorescence of the *nos*-GFP reporter plasmid was also monitored in the biofilm growth conditions, however no appreciable fluorescence was detected at the 24 hour time point tested when observed by confocal microscopy. This lack of fluorescence could be caused by a

signal too weak to be detected by the confocal microscope, or, alternatively, too few cells are expressing *nos* under these biofilm growth conditions, making them difficult to find and visualize by microscopy (data not shown).

The *nos* Mutant Produces a More Adherent Biofilm

To begin to appreciate whether *nos* is involved in regulating biofilm development in *S. aureus,* 24 hour static biofilm growth was assessed in UAMS-1, the *nos::*Erm mutant, and complement strains. This model of biofilm growth is primarily used to measure initial attachment and the early phases of biofilm development. The LIVE/DEAD stain (Invitrogen) utilized in this study is comprised of Syto 9 and propidium iodide, nucleic acid stains that differentiate between live (green) and dead (red) cells, respectively. The Syto 9 stains both live and dead bacteria, however the PI penetrates only dead or damaged bacteria, with the red stain fluorescence dominating the green fluorescence. Using this method of biofilm visualization, after 24 hours growth, the *nos* mutant consistently displayed qualitative differences in its overall thickness and structure compared to the wild-type and complement strains, in addition to a brighter green fluorescence (possibly due to more cells present or altered uptake of the Syto 9 dye)(Figure 3-9). Furthermore, COMSTAT and statistical analysis showed there is a subtle-yet-significant difference between the *nos* mutant and wild-type/complement strains in terms of average thickness (Figure 3-10A), biomass (Figure 3-10B) and the surface area to biomass ratio, which is used as an indicator of biofilm adaptability to environmental stresses [113] (Figure 3-10C). Specifically, the mutant is on average thicker than the wild-type strain, has a greater biomass, and a smaller surface area to biomass ratio. Collectively, these results indicate that the *nos* mutation affects biofilm adherence and architecture in the early phases of biofilm development.

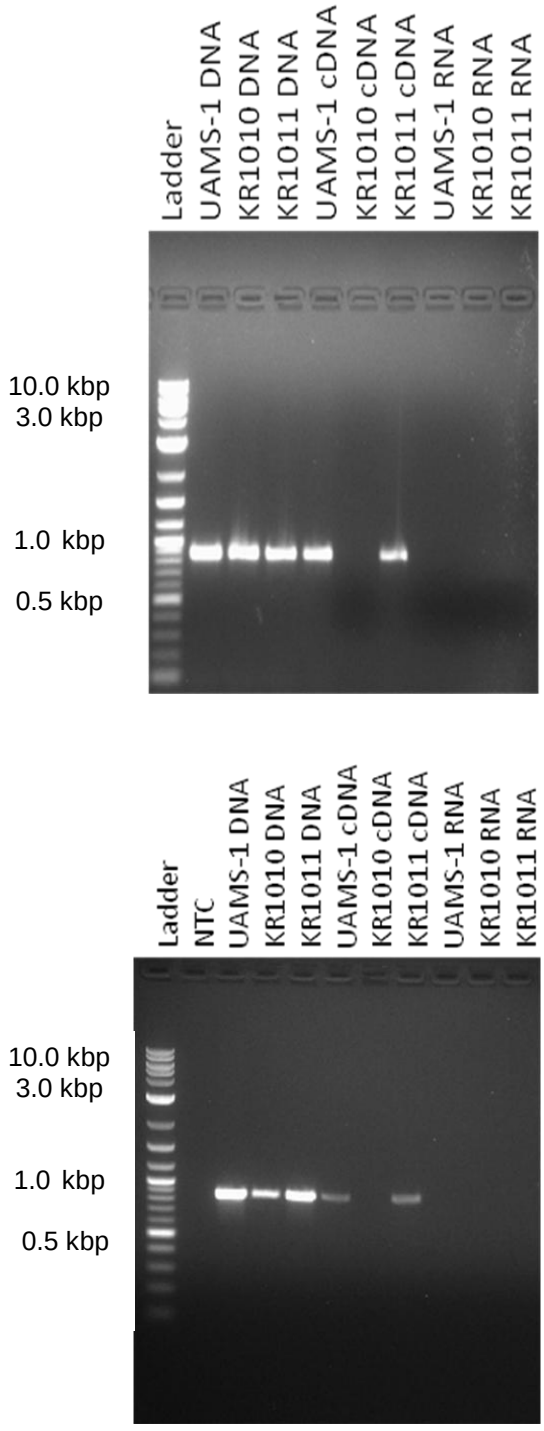

Figure 3-1. nos and SAR2008 are co-transcribed. Two representative experiments are depicted. For each gel, Lane 1 is a 2-log ladder. PCR reactions contain either 75 ng genomic DNA template, 75 ng cDNA template or 75 ng RNA template, respectively.

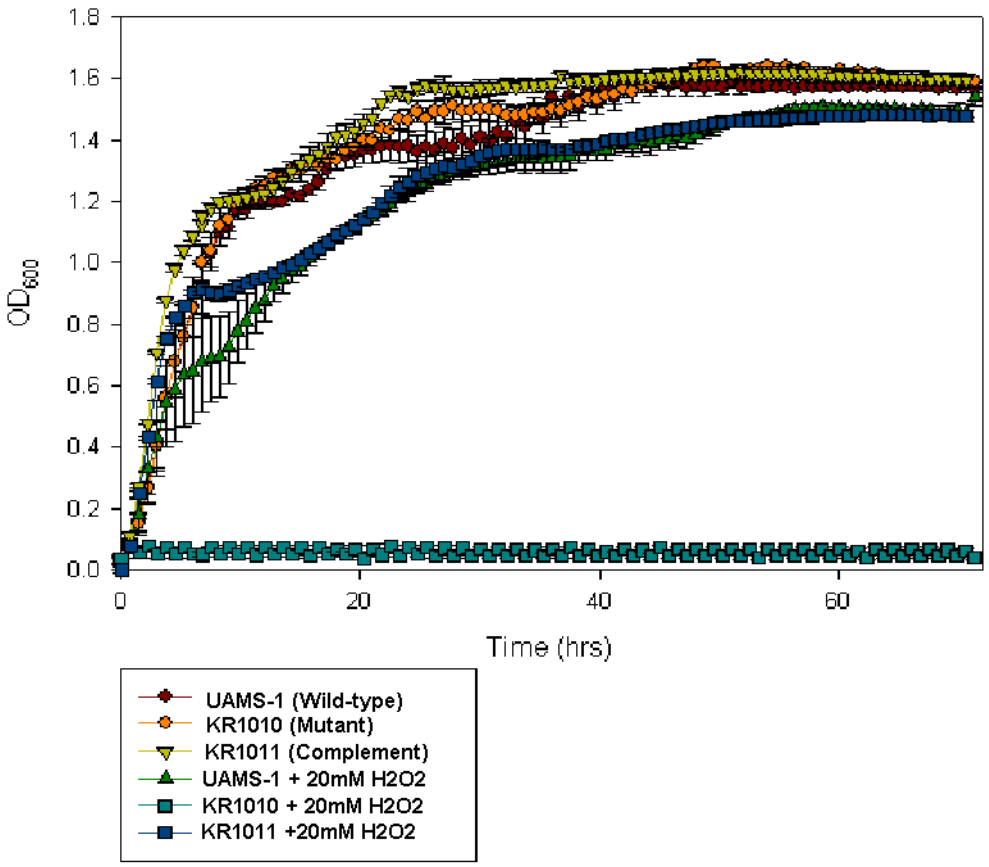

Figure 3-2. Growth of Wild-type, mutant and complement strains in TSB and TSB + 20mM H_2O_2 growth conditions.

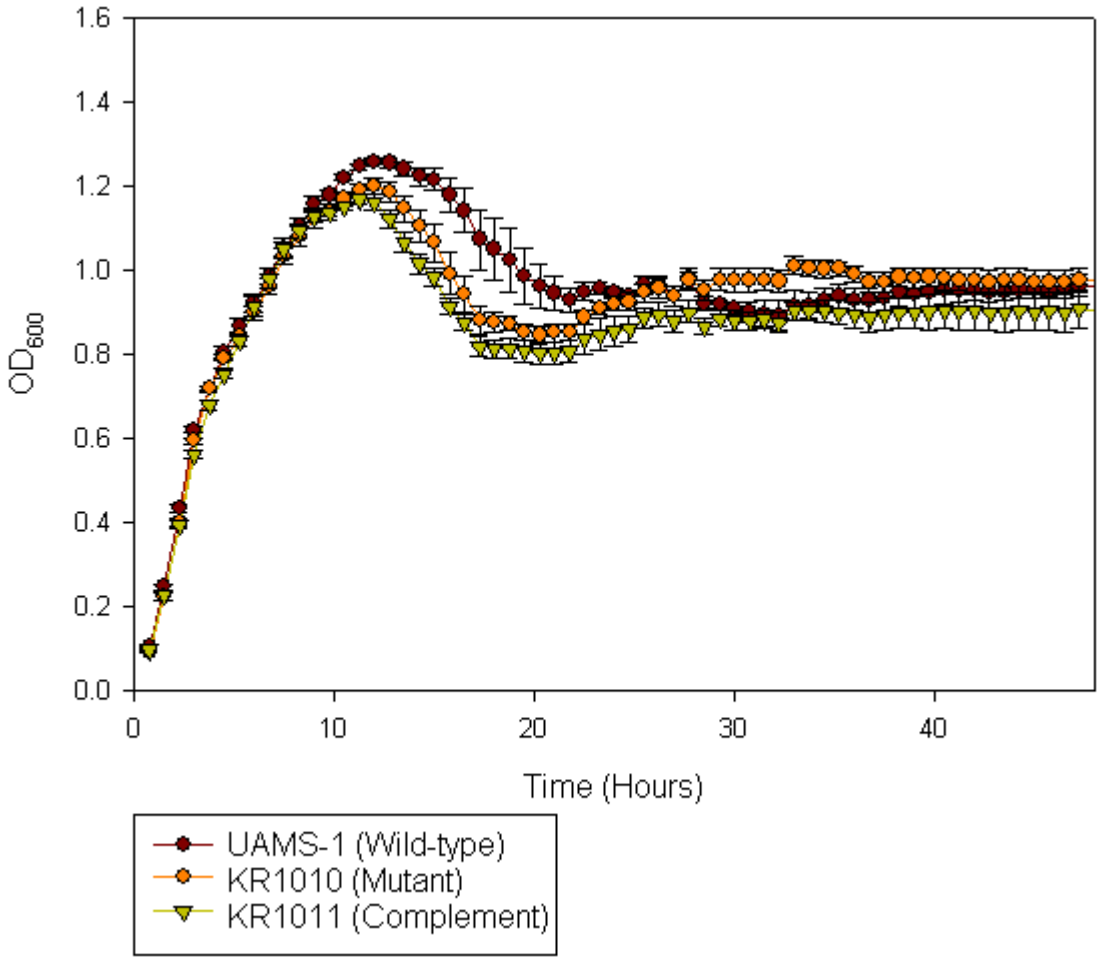

Figure 3-3. UAMS-1, KR1010, KR1011 growth in 3% TSB+ 3% NaCl+ 0.5% glucose medium for 48 hours.

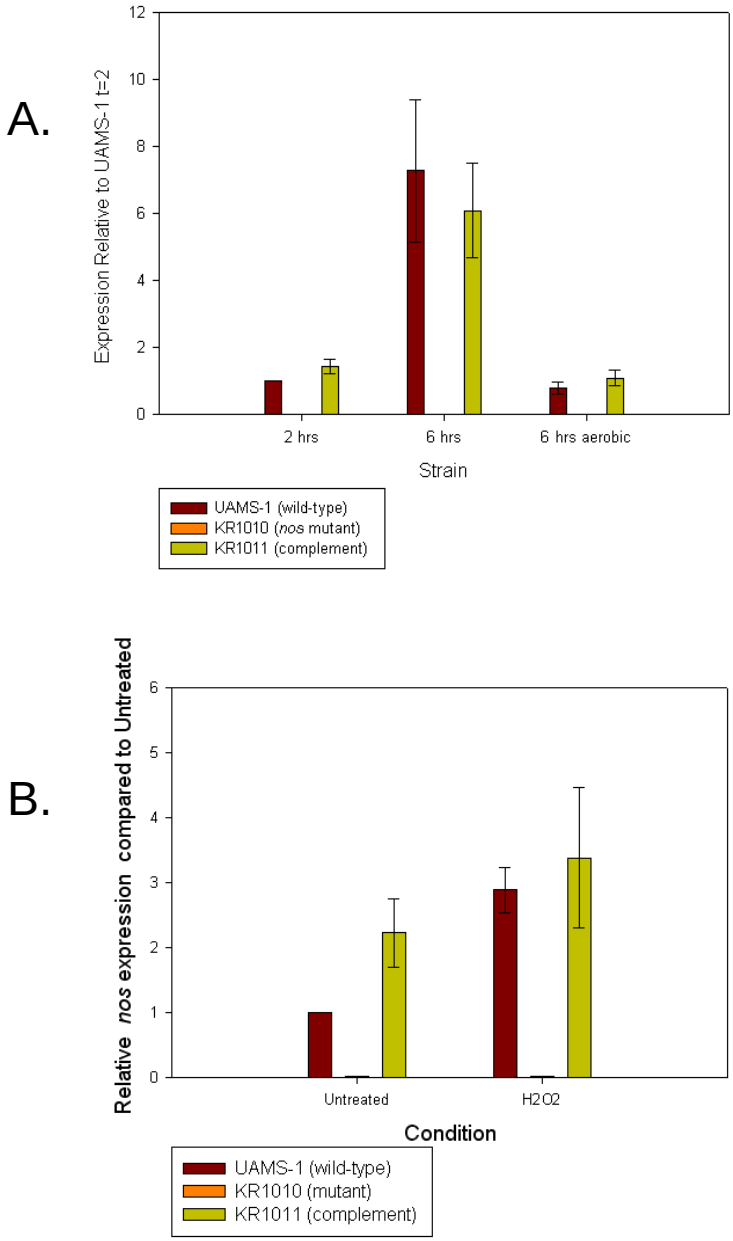

Figure 3-4. Expression of *nos* under (A) 2-and 6-hour low oxygen condition, 6 hours highly aerated (n=3) in addition to (B) treated and untreated with hydrogen peroxide as previously described (n=1). The hydrogen peroxide are normalized to the untreated under the same condition, while the other conditions are a fold increase as compared to 2 hours. There are no bars on the KR1010 (*nos* mutant) due to the absence of an amplification product.

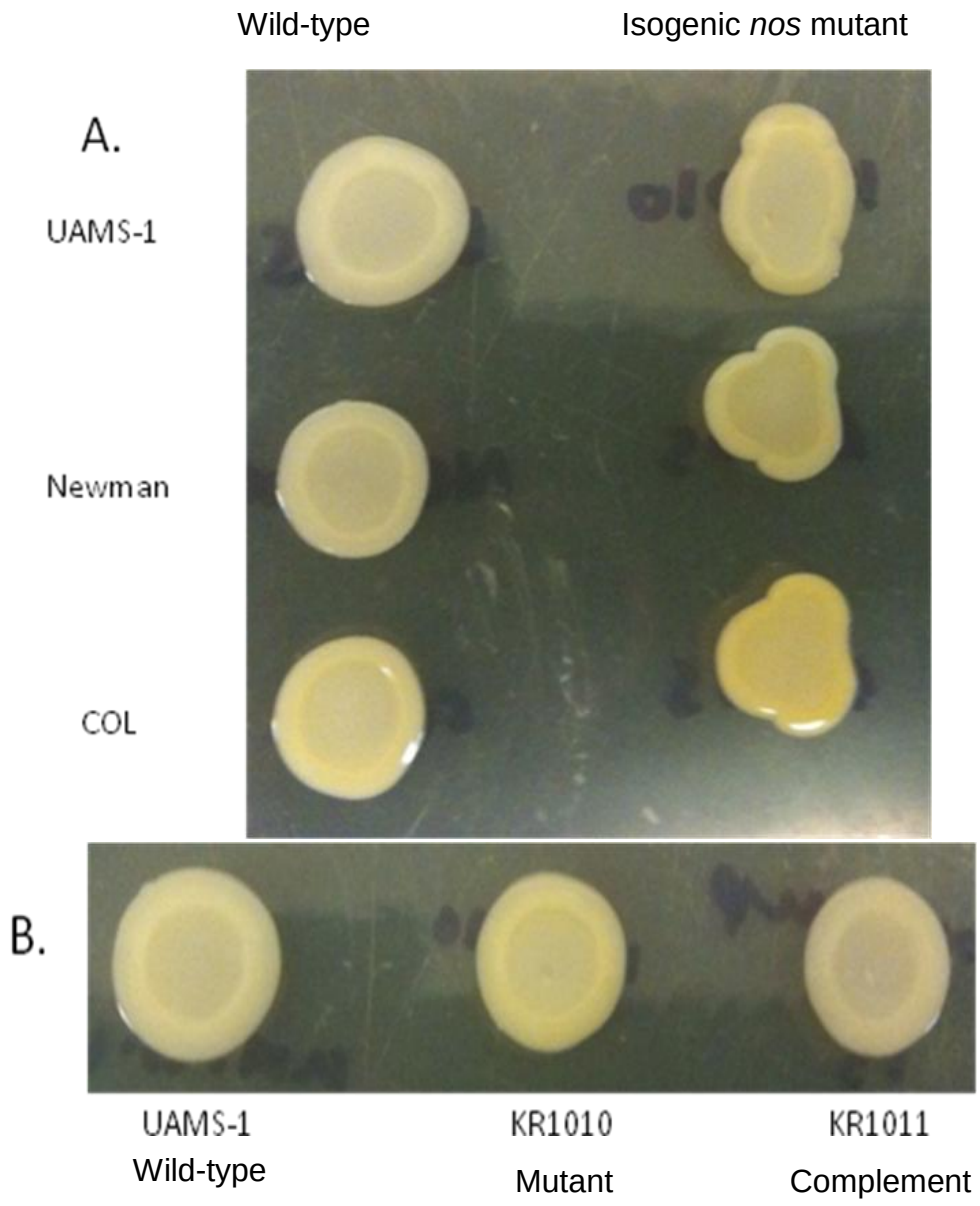

Figure 3-5. Increased pigment production in the *nos* mutant when grown on TSA plates. A) Increased pigment was observed in the *nos* mutant in 3 different *S. aureus* genetic backgrounds when cultured for 48 hours on TSA plates. B) Pigment production was increased in the *nos* mutant strain (KR1010) relative to UAMS-1 and was complemented back to parental phenotype in KR1011. Each picture is representative of 3 replicates

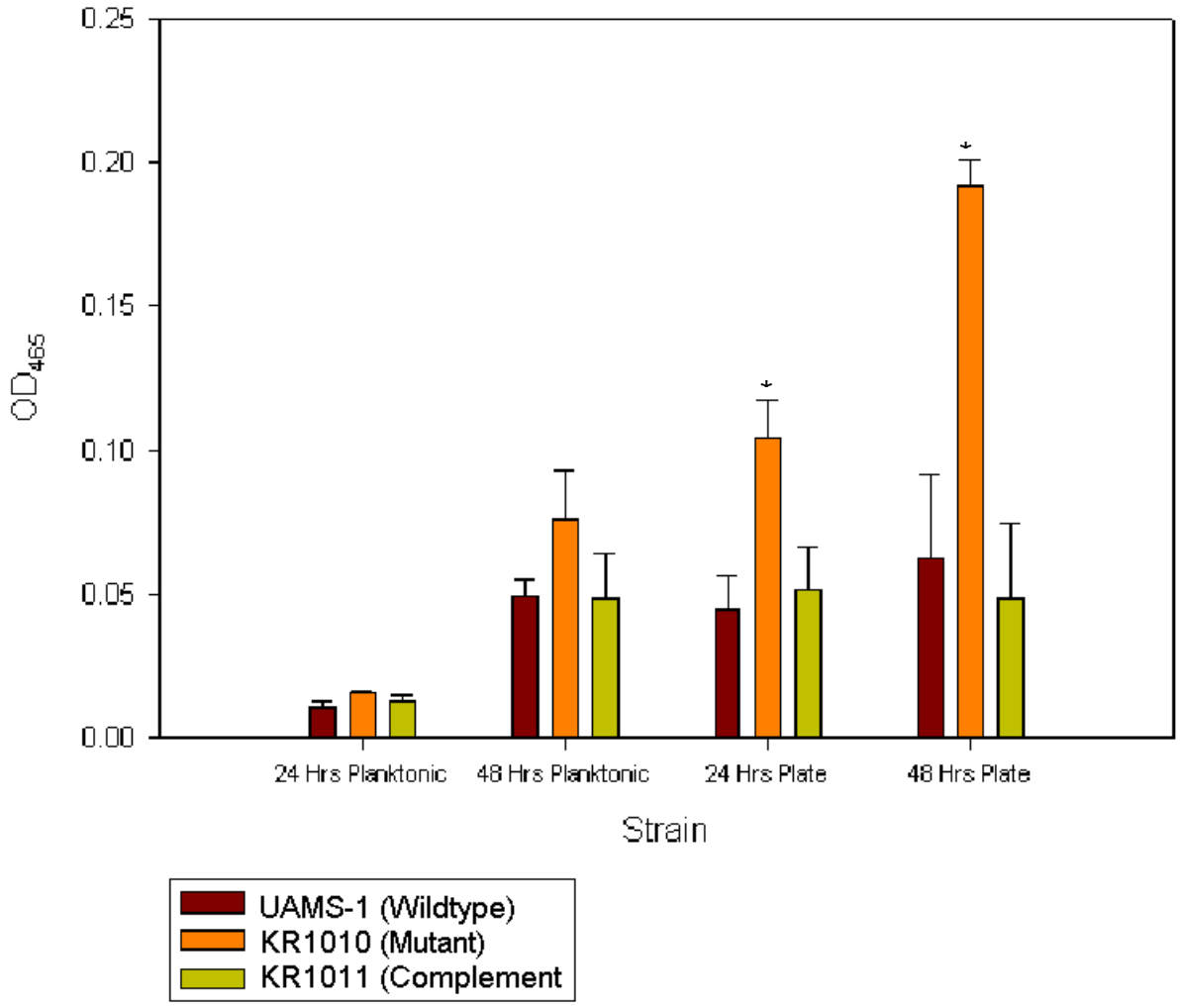

Figure 3-6. Total pigment concentration of *S. aureus nos* mutant. Asterisks represent statistically significant difference as described previously in the results. Results represent the average of 3 independent experiments.

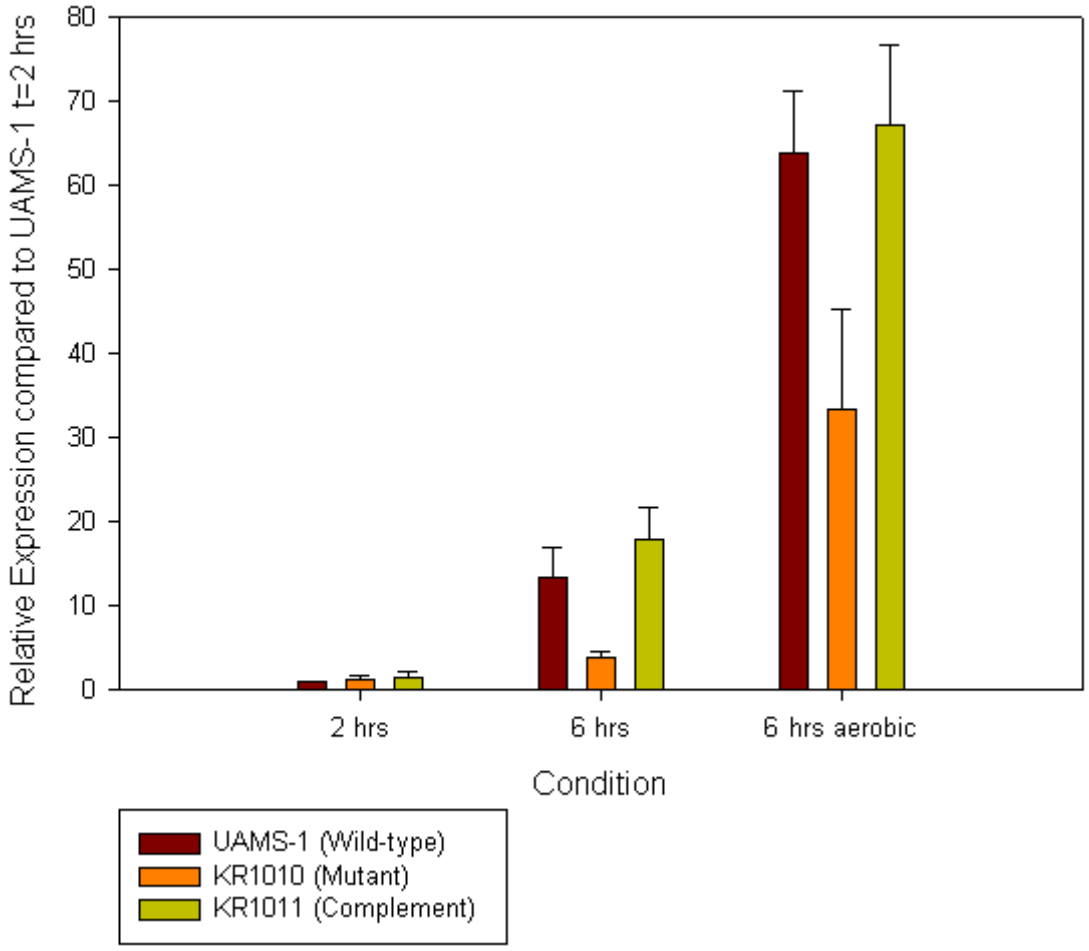

Figure 3-7. qRT-PCR reveals a decrease in *purH* expression in the *nos* mutant at the 6 hour time point under aerated and low oxygen growth. Results represent the average of three independent experiments.

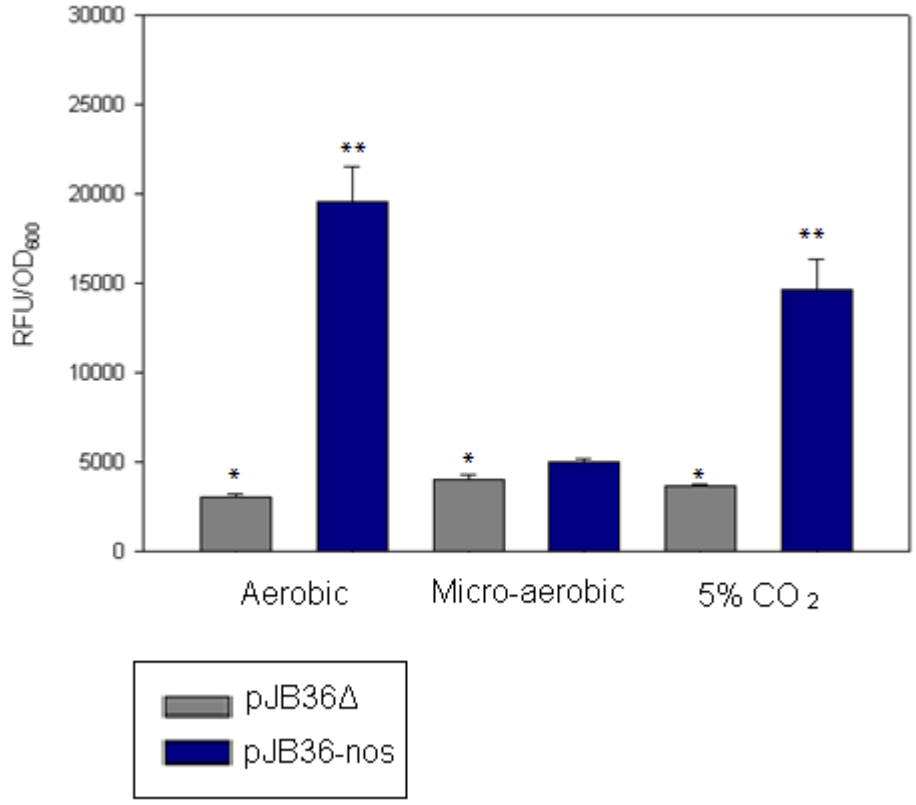

Figure 3-8. Expression of a *nos*-GFP reporter in UAMS-1 when grown on TSA plates under various environmental conditions. * = significant difference between delta and corresponding *nos* expression. ** = significant difference in respect to low oxygen. Data represent 3 independent experiments

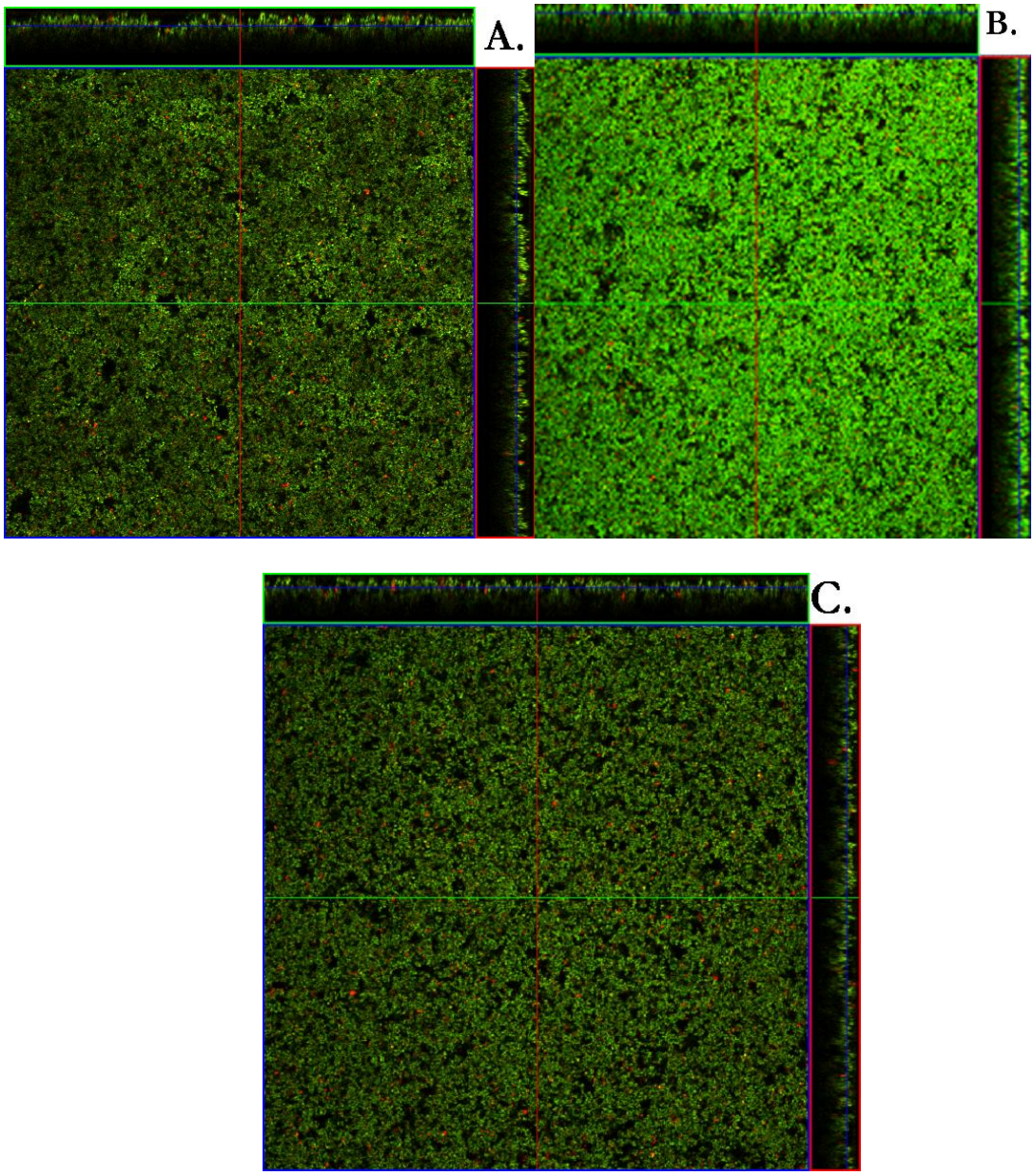

Figure 3-9. Representative orthogonal views of 24 hour static biofilms. The large square in each biofilm is the top down view whereas the side panels are orthogonal (side) views. The cells are stained with LIVE/DEAD stain where the red cells are dead or damaged and the green cells are live. A) UAMS-1, B) KR1010, C) KR1011. Images were acquire at 400x magnification by confocal microscopy, and are each representative of 18 random fields of view acquired in 3 independent experiments

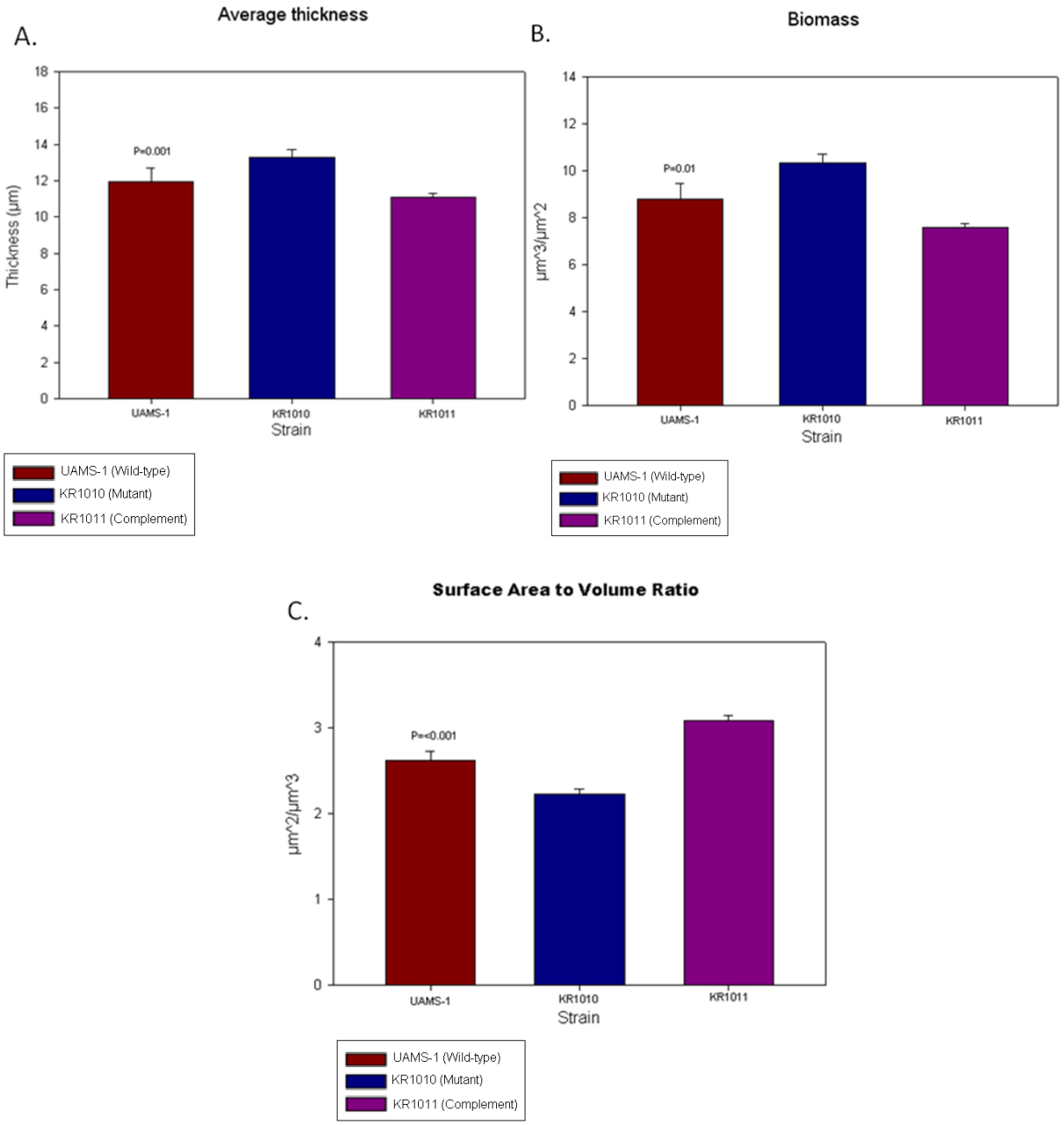

Figure 3-10. COMSTAT analysis reveals statistically significant (Student-Newman-Keuls test) differences between wild-type (UAMS-1) and *nos* mutant (KR1010), and the phenotype is complementable (KR1011). A) Average Thickness B) Biomass C) Surface Area to Volume Ratio. P-values are indicated on each graph. Data represents 18 measurements of each parameter acquired in 3 independent experiments.

CHAPTER 4
DISCUSSION

Role of *nos* in *S. aureus* Oxidative Stress

SAR2008, a putative prephenate dehydratase, is located 20bp downstream from the *nos* gene. This close proximity suggested it was probable this gene is cotranscribed with the *nos* gene. In agreement with this possibility, northern blotting of RNA with probes each specific for *nos* and *SAR2008* showed no hybridization in the *nos* mutant, but both probes each hybridized to a transcript of the same length in the wild-type strain, indicating they are co-transcribed (data not shown). Furthermore, PCR with primers amplifying a region 127bp downstream from the Erm cassette and 162bp downstream from the SAR2008 start codon show amplification in both the UAMS-1 (wild-type) and KR1010 (complement) cDNA, whereas the KR1010 (mutant) cDNA showed no amplification. This result also implies co-transcription of these two genes. Given that the *nos* mutation likely abrogates SAR2008 transcription, all phenotypes observed in this study are possibly due to the inactivation of one or both of these genes. Future work will be done to create and compare phenotypes of both a non-polar *nos* mutant and a non-polar SAR2008 mutant, to determine the specific contribution of each gene to the bacterium's oxidative stress response and biofilm development.

Co-transcription implies a potential working relationship between *nos* and SAR2008, the putative prephenate dehydratase, possibly involved in oxidative stress relief. Prephenate dehydratase is known to be involved in aromatic amino acid biosynthesis and catalyzes the decarboxylation of prephenate to phenylpyruvate [131]. Expression of this gene has been shown to be up-regulated in response to hydrogen peroxide in *S. aureus*, presumably due to co-transcription with *nos* [116]. Intriguingly,

phenylpyruvate has also been shown to have antioxidant capabilities through the nucelophilic attack of a monoprotonated hydrogen peroxide ion, which attacks the C-2 carbonyl group carbon center [132]. Given the genetic organization and co-transcription of *nos* and SAR2008, it is tempting to speculate that up-regulation of prephenate dehydratase expression during hydrogen peroxide stress may in itself be an anti-oxidant mechanism, by up-regulating production of phenylpyruvate. Alternatively, akin to the activation of catalase of endogenously produced NO by *nos* in *Bacillus,* perhaps SaNOS is responsible for activating the SAR2008 prephenate dehydratase enzyme in response to oxidative stress.

While there was not an observed difference under planktonic growth condition in either TSB and biofilm medium between the wild-type, *nos* mutant and complement strains, the addition of oxidative stress by means of hydrogen peroxide revealed an increased susceptibility of the *nos* mutant to H_2O_2 that was not observed in the wild-type or complement strains. This decreased tolerance suggests a potential role for SaNOS in oxidative stress relief, although it is unclear from these studies whether the specific NO-dependent mechanism previously observed in *Bacillus* (i.e. activation of an catalase, or preventing the Fenton reaction [96]) also holds true for *S. aureus nos*. A role for *nos* in oxidative stress relief is also supported by the increased pigment production observed in the *nos* mutant, in conjunction with the increased expression of the *nos* gene in the wild-type strain under these same growth conditions. These results suggest the *nos* mutant may be subject to additional oxidative stress compared to the wild-type strain, and may be compensating for this by overproducing carotenoid pigment. Conversely, the NO produced by the NOS enzyme may have a role in

signaling or regulating pigment production. Currently, our results cannot differentiate between the two possibilities.

These observations correlate to a paper by Lan et al. [130] looking at pigment mutants in *S. aureus,* and more specifically those involved in purine biosynthesis such as the protein PurH, which catalyzes the final steps in the biosynthesis of inosine monophosphate [133]. In the study by Lan et al., a *purH* mutant showed hyperpigmentation, decreased purine biosynthesis and decreased *nos* expression. Interestingly, this phenotype is in accordance with the *nos* mutant characterized in this study, as this mutant also displayed increased pigment production and decreased expression of *nos* and *purH.* These observations may suggest a mechanism in which increased oxidative stress on the cells alters *S. aureus* metabolism in favor of NADPH production, and pyridine nucleotides which are consumed by many antioxidant enzymatic systems [134]. Although these results suggest a relationship and/or feedback mechanism between *nos,* purine biosynthesis and pigment production, the exact interactions are currently unknown and require further investigation.

The Contribution of *nos* under Biofilm Conditions

While a role for *nos* as an antioxidant mechanism seems likely, *nos* has also been shown to be expressed either at a basal level under all growth conditions, or alternatively, is expressed by only a subpopulation of cells, rendering *nos* expression difficult. To determine if the *nos* expression is localized or expressed at a basal level, future studies will use the *nos*-GFP-reporter and flow cytometry to determine if higher fluorescence only occurs in a subpopulation of cells under various growth conditions. Furthermore, NO can be visualized via a fluorescent stain, DAF-FM, which would show whether the NO is present uniformly throughout the cell population or localized to a

more specific area. Nonetheless, *nos* expression at basal levels throughout the bacterial population or, alternatively, by a subpopulation of cells suggests, potentially, an additional role of *nos,* perhaps in terms of NO production for cell-signaling, as previously mentioned [15,80,81].

Under static biofilm conditions the *nos* mutant has a more attached, robust biofilm. It is on average thicker, with a lower surface area to biomass ratio when compared to the wild-type and complement strains. This decreased ratio is indicative of the biofilm's ability to adapt to surroundings and the nutrient and oxygen availability within the heterogeneous biofilm, suggesting perhaps this biofilm is less responsive to environmental signals, and potentially less fit. The higher biomass and thickness of the mutant biofilm shows there may be a relationship between endogenously produced nitric oxide and biofilm attachment (with less NO resulting in more attachment as previously observed in *Neisseria* biofilms [74]). While the differences between the wild-type, mutant and complement strains were subtle, this may be due to other sources of NO (disproportionation and *nar*), or due to the nitric-oxide reductase (*nor*) gene unique to UAMS-1 and related strains. The presence of *nor* in this strain may minimize the net levels of endogenous NO in the wild-type strain and therefore may, in part, explain the subtle biofilm phenotype of the *nos* mutant. A *nos/nor* double mutant is currently being created to test if there is a more dramatic phenotypic change in the double mutant compared to each single mutant and wild-type strain. Given that the biofilm experiments performed in this study focused on the attachment phase, further work will need to be done to establish a relationship, if any, between NO/*nos* and biofilm dispersal.

Sensitivity to hydrogen peroxide may also be related to biofilm development and signaling cell dispersal. *In vivo, S. aureus* biofilms likely encounter the innate immune system through interactions with neutrophil and macrophage respiratory bursts, which would release a combination of oxidative antimicrobials. Given that *nos* expression is up-regulated in response to hydrogen peroxide [116], it is tempting to speculate that NO production by *nos* may function to trigger cell dispersal and/or other adaptive responses. Potentially, endogenously produced NO via *nos* is expressed at a basal level in the early stages of biofilm development, allowing for attachment. Presumably, in the *nos* mutant, further decreasing NO production may have allowed for increased attachment of the biofilm relative to wild-type strain. In response to a respiratory burst, or accumulation of oxidative stresses in highly populated areas of the biofilm, *nos* expression, already active on a basal level, could be induced, signaling cells within the biofilm to disperse and colonize new areas. This model as of yet is just a model, and the NO contribution of *nos* (in the wild-type, mutant and complement strains), as compared to other potential endogenous sources of NO (*nar* and disproportionation), in addition to interactions between neutrophils and wild-type UAMS-1, *nos* mutant and complement biofilms have yet to be tested (Figure 4-1).

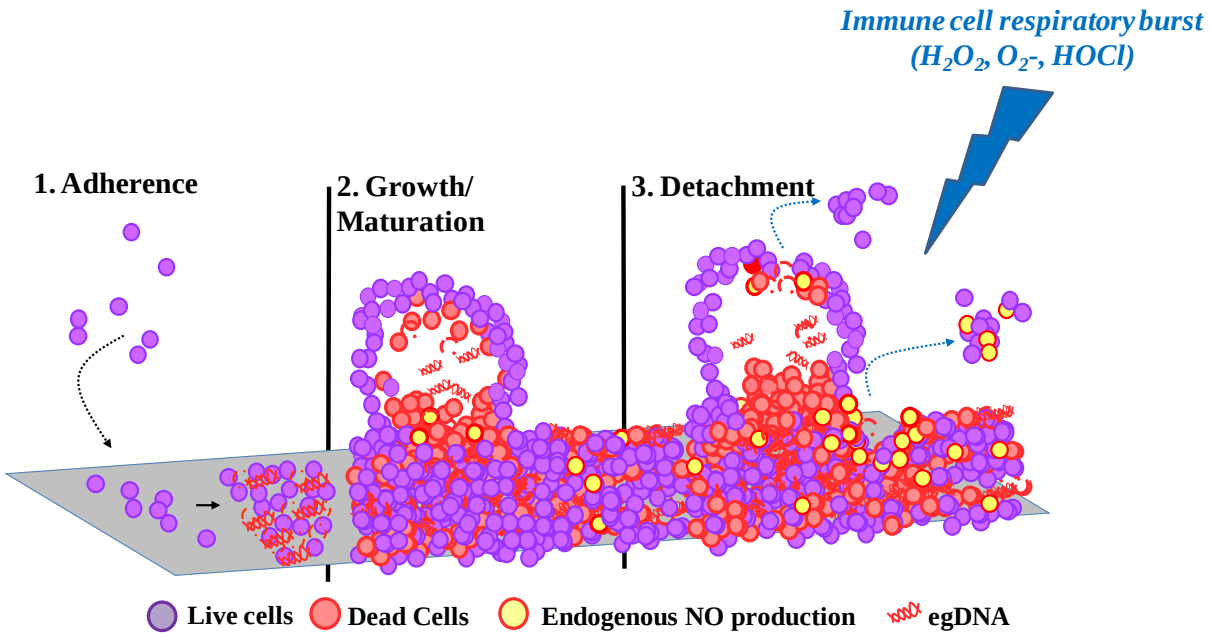

Figure 4-1. A potential model for the role of *S. aureus nos* gene in biofilm development.

CHAPTER 5
CONCLUSIONS

Nitric oxide is an important signaling molecule in eukaryotes, prokaryotes and archaea. While the role of nitric oxide synthases in eukaryotes and some bacteria is known, there are still numerous bacteria where the specific role of their nitric oxide synthase has yet to be elucidated. The work presented in this thesis has elaborated on a possible role for this enzyme in the pernicious human pathogen *S. aureus*, one of the leading causes of bacterial infection worldwide.

Under planktonic conditions the *nos* gene has a role in dealing with oxidative stress. It is up-regulated under hydrogen peroxide stress and it is also up-regulated in the later phases of growth when there is increased cell population, potentially due to metabolic changes or increased cell density, suggesting a possible additional role for *nos* in cell-signaling. There is also a correlation between *nos* down-regulation and pigment production, suggesting it stresses the cells and forces them to compensate by producing more of the antioxidant carotenoids. Alternatively, *nos* is involved in the regulation of carotenoid pigment production, potentially either acting directly on the enzyme or indirectly via cell-signaling. Its expression is also up-regulated under TSA growth condition, which may relate to a role in biofilm formation given that cells are growing together as a multicellular “colony”.

When the role of *nos* under static biofilm growth conditions was examined, there was a subtle but very reproducible difference in biofilm structure. The *nos* mutant biofilm was a more attached biofilm, but possibly with less potential for interacting with environmental signals and/or acquisition of nutrients due to a decreased biofilm to surface area ratio [113]. This phenotype suggests a potential role for nitric oxide

produced by SaNOS in regulating attachment and other unknown events during the early phases of biofilm development. This nitric oxide production could be localized to certain populations of cells within the biofilm, or induced in response to stress caused by the immune system such as from the respiratory burst of immune cells. While the exact targets of SaNOS are not yet known, these results, pending animal model testing, suggest a method for which the already virulent *S. aureus* may be able to avoid immune system destruction and increase infection persistence within the host.

APPENDIX A
SAMPLE CALCULATION DETERMINING QRT-PCR EXPRESSION OF *NOS*

Table A-1. One set of qRT-PCR numbers being used to calculate the expression by the $2^{-\Delta\Delta CT}$ method (Livak method).

Sample	**C_T *nos* (Target)**	**C_T σ^{70} (Reference)**
UAMS-1 t=2 (calibrator)	20.94	20.59
UAMS-1 t=6 low oxygen (test)	18.54	20.87

Figure A-1. Sample calculation for the expression levels of *nos* in comparison to σ^{70} using the $2^{-\Delta\Delta CT}$ method (Livak method). For this calculation, the σ^{70} is the reference gene and UAMS-1 t=2 expression is considered the calibrator.

$$\Delta C_{T(\text{UAMS-1 t=2})}=20.94-20.59=0.35$$

$$\Delta C_{T(\text{UAMS-1 t=6})}=18.59-20.87=-2.33$$

$$\Delta\Delta C_T=\Delta C_{T(\text{UAMS-1 t=6})}-\Delta C_{T(\text{UAMS-1 t=2})}$$

$$=-2.33-0.35=-2.68$$

$$2^{-\Delta\Delta CT}=2^{-(-2.68)}=6.41$$

In this example, UAMS-1 at t=6 hours is expressing *nos* at a 6.41-fold higher level than UAMS-1 at t=2 hours.

For all values presented in Figure 3-4 (Part A) and Figure 3-7, UAMS-1 t=2 was always used as the calibrator. For all values presented in Figure 3-4 (Part B), UAMS-1 untreated was always used as the calibrator.

LIST OF REFERENCES

1. Wilkinson B (1997) The staphylococci in human disease; Crossley KB AG, editor. New York: Churchill Livingstone. 37 p.

2. Schaberg DR, Zervos MJ (1986) Intergeneric and interspecies gene exchange in gram-positive cocci. Antimicrob Agents Chemother 30: 817-822.

3. Novick R (1990) Molecular biology of the staphylococci; RP N, editor. New York: VCH. 37 p.

4. Fuchs S, Pane-Farre J, Kohler C, Hecker M, Engelmann S (2007) Anaerobic gene expression in Staphylococcus aureus. J Bacteriol 189: 4275-4289.

5. Liu GY, Essex A, Buchanan JT, Datta V, Hoffman HM, et al. (2005) Staphylococcus aureus golden pigment impairs neutrophil killing and promotes virulence through its antioxidant activity. J Exp Med 202: 209-215.

6. Deleo FR, Otto M, Kreiswirth BN, Chambers HF (2010) Community-associated meticillin-resistant Staphylococcus aureus. Lancet 375: 1557-1568.

7. Lowy FD (2003) Antimicrobial resistance: the example of Staphylococcus aureus. J Clin Invest 111: 1265-1273.

8. Gordon RJ, Lowy FD (2008) Pathogenesis of methicillin-resistant Staphylococcus aureus infection. Clin Infect Dis 46 Suppl 5: S350-359.

9. Meziane-Cherif D, Saul FA, Moubareck C, Weber P, Haouz A, et al. (2010) Molecular basis of vancomycin-dependence in VanA-type Staphylococcus aureus VRSA-9. J Bacteriol.

10. Cheung AL, Bayer AS, Zhang G, Gresham H, Xiong YQ (2004) Regulation of virulence determinants in vitro and in vivo in Staphylococcus aureus. FEMS Immunol Med Microbiol 40: 1-9.

11. Vuong C, Saenz HL, Gotz F, Otto M (2000) Impact of the agr quorum-sensing system on adherence to polystyrene in Staphylococcus aureus. J Infect Dis 182: 1688-1693.

12. Kong KF, Vuong C, Otto M (2006) Staphylococcus quorum sensing in biofilm formation and infection. Int J Med Microbiol 296: 133-139.

13. Zhang L, Gray L, Novick RP, Ji G (2002) Transmembrane topology of AgrB, the protein involved in the post-translational modification of AgrD in Staphylococcus aureus. J Biol Chem 277: 34736-34742.

14. Yarwood JM, Bartels DJ, Volper EM, Greenberg EP (2004) Quorum sensing in Staphylococcus aureus biofilms. J Bacteriol 186: 1838-1850.

15. Barraud N, Schleheck D, Klebensberger J, Webb JS, Hassett DJ, et al. (2009) Nitric oxide signaling in Pseudomonas aeruginosa biofilms mediates phosphodiesterase activity, decreased cyclic di-GMP levels, and enhanced dispersal. J Bacteriol 191: 7333-7342.

16. Kumar CG, Anand SK (1998) Significance of microbial biofilms in food industry: a review. Int J Food Microbiol 42: 9-27.

17. Yang J, Bos R, Belder GF, Engel J, Busscher HJ (1999) Deposition of Oral Bacteria and Polystyrene Particles to Quartz and Dental Enamel in a Parallel Plate and Stagnation Point Flow Chamber. J Colloid Interface Sci 220: 410-418.

18. Rijnaarts HH, Norde W, Bouwer EJ, Lyklema J, Zehnder AJ (1993) Bacterial Adhesion under Static and Dynamic Conditions. Appl Environ Microbiol 59: 3255-3265.

19. Hood SK, Zottola EA (1997) Adherence to stainless steel by foodborne microorganisms during growth in model food systems. Int J Food Microbiol 37: 145-153.

20. Whitehead KA, Rogers D, Colligon J, Wright C, Verran J (2006) Use of the atomic force microscope to determine the effect of substratum surface topography on the ease of bacterial removal. Colloids Surf B Biointerfaces 51: 44-53.

21. Palmer J, Flint S, Brooks J (2007) Bacterial cell attachment, the beginning of a biofilm. J Ind Microbiol Biotechnol 34: 577-588.

22. Boles BR, Horswill AR (2008) Agr-mediated dispersal of Staphylococcus aureus biofilms. PLoS Pathog 4: e1000052.

23. Otto M (2008) Staphylococcal biofilms. Curr Top Microbiol Immunol 322: 207-228.

24. Rice KC, Mann EE, Endres JL, Weiss EC, Cassat JE, et al. (2007) The cidA murein hydrolase regulator contributes to DNA release and biofilm development in Staphylococcus aureus. Proc Natl Acad Sci U S A 104: 8113-8118.

25. Mann EE, Rice KC, Boles BR, Endres JL, Ranjit D, et al. (2009) Modulation of eDNA release and degradation affects Staphylococcus aureus biofilm maturation. PLoS One 4: e5822.

26. Patti JM, Allen BL, McGavin MJ, Hook M (1994) MSCRAMM-mediated adherence of microorganisms to host tissues. Annu Rev Microbiol 48: 585-617.

27. O'Neill E, Pozzi C, Houston P, Humphreys H, Robinson DA, et al. (2008) A novel Staphylococcus aureus biofilm phenotype mediated by the fibronectin-binding proteins, FnBPA and FnBPB. J Bacteriol 190: 3835-3850.

28. Ulrich M, Bastian M, Cramton SE, Ziegler K, Pragman AA, et al. (2007) The staphylococcal respiratory response regulator SrrAB induces ica gene transcription and polysaccharide intercellular adhesin expression, protecting Staphylococcus aureus from neutrophil killing under anaerobic growth conditions. Mol Microbiol 65: 1276-1287.

29. Kogan G, Sadovskaya I, Chaignon P, Chokr A, Jabbouri S (2006) Biofilms of clinical strains of Staphylococcus that do not contain polysaccharide intercellular adhesin. FEMS Microbiol Lett 255: 11-16.

30. Izano EA, Amarante MA, Kher WB, Kaplan JB (2008) Differential roles of poly-N-acetylglucosamine surface polysaccharide and extracellular DNA in Staphylococcus aureus and Staphylococcus epidermidis biofilms. Appl Environ Microbiol 74: 470-476.

31. Chaignon P, Sadovskaya I, Ragunah C, Ramasubbu N, Kaplan JB, et al. (2007) Susceptibility of staphylococcal biofilms to enzymatic treatments depends on their chemical composition. Appl Microbiol Biotechnol 75: 125-132.

32. Lauderdale KJ, Malone CL, Boles BR, Morcuende J, Horswill AR (2010) Biofilm dispersal of community-associated methicillin-resistant Staphylococcus aureus on orthopedic implant material. J Orthop Res 28: 55-61.

33. Novick RP, Ross HF, Projan SJ, Kornblum J, Kreiswirth B, et al. (1993) Synthesis of staphylococcal virulence factors is controlled by a regulatory RNA molecule. EMBO J 12: 3967-3975.

34. Traber KE, Lee E, Benson S, Corrigan R, Cantera M, et al. (2008) agr function in clinical Staphylococcus aureus isolates. Microbiology 154: 2265-2274.

35. Geisinger E, Muir TW, Novick RP (2009) agr receptor mutants reveal distinct modes of inhibition by staphylococcal autoinducing peptides. Proc Natl Acad Sci U S A 106: 1216-1221.

36. Yarwood JM, Paquette KM, Tikh IB, Volper EM, Greenberg EP (2007) Generation of virulence factor variants in Staphylococcus aureus biofilms. J Bacteriol 189: 7961-7967.

37. Laarman A, Milder F, van Strijp J, Rooijakkers S (2010) Complement inhibition by gram-positive pathogens: molecular mechanisms and therapeutic implications. J Mol Med 88: 115-120.

38. Voyich JM, Braughton KR, Sturdevant DE, Whitney AR, Said-Salim B, et al. (2005) Insights into mechanisms used by Staphylococcus aureus to avoid destruction by human neutrophils. J Immunol 175: 3907-3919.

39. del Pozo JL, Patel R (2007) The challenge of treating biofilm-associated bacterial infections. Clin Pharmacol Ther 82: 204-209.

40. Bokarewa MI, Jin T, Tarkowski A (2006) Staphylococcus aureus: Staphylokinase. Int J Biochem Cell Biol 38: 504-509.

41. Foster TJ (2005) Immune evasion by staphylococci. Nat Rev Microbiol 3: 948-958.

42. Cunnion KM, Hair PS, Buescher ES (2004) Cleavage of complement C3b to iC3b on the surface of Staphylococcus aureus is mediated by serum complement factor I. Infect Immun 72: 2858-2863.

43. Cunnion KM, Buescher ES, Hair PS (2005) Serum complement factor I decreases Staphylococcus aureus phagocytosis. J Lab Clin Med 146: 279-286.

44. Clements MO, Watson SP, Foster SJ (1999) Characterization of the major superoxide dismutase of Staphylococcus aureus and its role in starvation survival, stress resistance, and pathogenicity. J Bacteriol 181: 3898-3903.

45. Das D, Bishayi B (2009) Staphylococcal catalase protects intracellularly survived bacteria by destroying H2O2 produced by the murine peritoneal macrophages. Microb Pathog 47: 57-67.

46. Amin VM, Olson NF (1968) Influence of catalase activity on resistance of coagulase-positive staphylococci to hydrogen peroxide. Appl Microbiol 16: 267-270.

47. Nizet V (2007) Understanding how leading bacterial pathogens subvert innate immunity to reveal novel therapeutic targets. J Allergy Clin Immunol 120: 13-22.

48. Otto M (2006) Bacterial evasion of antimicrobial peptides by biofilm formation. Curr Top Microbiol Immunol 306: 251-258.

49. Mittal R, Aggarwal S, Sharma S, Chhibber S, Harjai K (2009) Contribution of macrophage secretory products to urovirulence of Pseudomonas aeruginosa. FEMS Immunol Med Microbiol 57: 156-164.

50. Jesaitis AJ, Franklin MJ, Berglund D, Sasaki M, Lord CI, et al. (2003) Compromised host defense on Pseudomonas aeruginosa biofilms: characterization of neutrophil and biofilm interactions. J Immunol 171: 4329-4339.

51. Crane BR, Sudhamsu J, Patel BA (2010) Bacterial nitric oxide synthases. Annu Rev Biochem 79: 445-470.

52. Bryan NS, Bian K, Murad F (2009) Discovery of the nitric oxide signaling pathway and targets for drug development. Front Biosci 14: 1-18.

53. Broillet MC (1999) S-nitrosylation of proteins. Cell Mol Life Sci 55: 1036-1042.

54. Ischiropoulos H (2009) Protein tyrosine nitration--an update. Arch Biochem Biophys 484: 117-121.

55. Sessa WC (1994) The nitric oxide synthase family of proteins. J Vasc Res 31: 131-143.

56. Raman CS, Li H, Martasek P, Kral V, Masters BS, et al. (1998) Crystal structure of constitutive endothelial nitric oxide synthase: a paradigm for pterin function involving a novel metal center. Cell 95: 939-950.

57. Fischmann TO, Hruza A, Niu XD, Fossetta JD, Lunn CA, et al. (1999) Structural characterization of nitric oxide synthase isoforms reveals striking active-site conservation. Nat Struct Biol 6: 233-242.

58. Bredt DS, Snyder SH (1992) Nitric oxide, a novel neuronal messenger. Neuron 8: 3-11.

59. Johnson EG, Sparks JP, Dzikovski B, Crane BR, Gibson DM, et al. (2008) Plant-pathogenic Streptomyces species produce nitric oxide synthase-derived nitric oxide in response to host signals. Chem Biol 15: 43-50.

60. Spiro S (2008) Metalloregulatory proteins and nitric oxide signalling in bacteria. Biochem Soc Trans 36: 1160-1164.

61. Kimura H, Mittal CK, Murad F (1975) Activation of guanylate cyclase from rat liver and other tissues by sodium azide. J Biol Chem 250: 8016-8022.

62. Kimura H, Murad F (1975) Two forms of guanylate cyclase in mammalian tissues and possible mechanisms for their regulation. Metabolism 24: 439-445.

63. Koesling D, Friebe A (1999) Soluble guanylyl cyclase: structure and regulation. Rev Physiol Biochem Pharmacol 135: 41-65.

64. Richardson AR, Dunman PM, Fang FC (2006) The nitrosative stress response of Staphylococcus aureus is required for resistance to innate immunity. Mol Microbiol 61: 927-939.

65. Ye RW, Tao W, Bedzyk L, Young T, Chen M, et al. (2000) Global gene expression profiles of Bacillus subtilis grown under anaerobic conditions. J Bacteriol 182: 4458-4465.

66. Nakano MM (2002) Induction of ResDE-dependent gene expression in Bacillus subtilis in response to nitric oxide and nitrosative stress. J Bacteriol 184: 1783-1787.

67. Spiro S (2007) Regulators of bacterial responses to nitric oxide. FEMS Microbiol Rev 31: 193-211.

68. Beaumont HJ, Lens SI, Reijnders WN, Westerhoff HV, van Spanning RJ (2004) Expression of nitrite reductase in Nitrosomonas europaea involves NsrR, a novel nitrite-sensitive transcription repressor. Mol Microbiol 54: 148-158.

69. Bodenmiller DM, Spiro S (2006) The yjeB (nsrR) gene of Escherichia coli encodes a nitric oxide-sensitive transcriptional regulator. J Bacteriol 188: 874-881.

70. Nakano MM, Geng H, Nakano S, Kobayashi K (2006) The nitric oxide-responsive regulator NsrR controls ResDE-dependent gene expression. J Bacteriol 188: 5878-5887.

71. Membrillo-Hernandez J, Coopamah MD, Channa A, Hughes MN, Poole RK (1998) A novel mechanism for upregulation of the Escherichia coli K-12 hmp (flavohaemoglobin) gene by the 'NO releaser', S-nitrosoglutathione: nitrosation of homocysteine and modulation of MetR binding to the glyA-hmp intergenic region. Mol Microbiol 29: 1101-1112.

72. Schlag S, Nerz C, Birkenstock TA, Altenberend F, Gotz F (2007) Inhibition of staphylococcal biofilm formation by nitrite. J Bacteriol 189: 7911-7919.

73. Barraud N, Hassett DJ, Hwang SH, Rice SA, Kjelleberg S, et al. (2006) Involvement of nitric oxide in biofilm dispersal of Pseudomonas aeruginosa. J Bacteriol 188: 7344-7353.

74. Falsetta ML, McEwan AG, Jennings MP, Apicella MA (2010) Anaerobic metabolism occurs in the substratum of gonococcal biofilms and may be sustained in part by nitric oxide. Infect Immun 78: 2320-2328.

75. Sudhamsu J, Crane BR (2009) Bacterial nitric oxide synthases: what are they good for? Trends Microbiol 17: 212-218.

76. Marletta MA (1993) Nitric oxide synthase structure and mechanism. J Biol Chem 268: 12231-12234.

77. Marletta MA, Hurshman AR, Rusche KM (1998) Catalysis by nitric oxide synthase. Curr Opin Chem Biol 2: 656-663.

78. Stuehr DJ, Santolini J, Wang ZQ, Wei CC, Adak S (2004) Update on mechanism and catalytic regulation in the NO synthases. J Biol Chem 279: 36167-36170.

79. Griffith OW, Stuehr DJ (1995) Nitric oxide synthases: properties and catalytic mechanism. Annu Rev Physiol 57: 707-736.

80. Crane BR, Arvai AS, Gachhui R, Wu C, Ghosh DK, et al. (1997) The structure of nitric oxide synthase oxygenase domain and inhibitor complexes. Science 278: 425-431.

81. Crane BR, Arvai AS, Ghosh DK, Wu C, Getzoff ED, et al. (1998) Structure of nitric oxide synthase oxygenase dimer with pterin and substrate. Science 279: 2121-2126.

82. Wang ZQ, Wei CC, Sharma M, Pant K, Crane BR, et al. (2004) A conserved Val to Ile switch near the heme pocket of animal and bacterial nitric-oxide synthases helps determine their distinct catalytic profiles. J Biol Chem 279: 19018-19025.

83. Sono M, Roach MP, Coulter ED, Dawson JH (1996) Heme-Containing Oxygenases. Chem Rev 96: 2841-2888.

84. Pant K, Bilwes AM, Adak S, Stuehr DJ, Crane BR (2002) Structure of a nitric oxide synthase heme protein from Bacillus subtilis. Biochemistry 41: 11071-11079.

85. Alderton WK, Cooper CE, Knowles RG (2001) Nitric oxide synthases: structure, function and inhibition. Biochem J 357: 593-615.

86. Hendriks J, Oubrie A, Castresana J, Urbani A, Gemeinhardt S, et al. (2000) Nitric oxide reductases in bacteria. Biochim Biophys Acta 1459: 266-273.

87. Gusarov I, Starodubtseva M, Wang ZQ, McQuade L, Lippard SJ, et al. (2008) Bacterial nitric-oxide synthases operate without a dedicated redox partner. J Biol Chem 283: 13140-13147.

88. Buddha MR, Keery KM, Crane BR (2004) An unusual tryptophanyl tRNA synthetase interacts with nitric oxide synthase in Deinococcus radiodurans. Proc Natl Acad Sci U S A 101: 15881-15886.

89. Adak S, Bilwes AM, Panda K, Hosfield D, Aulak KS, et al. (2002) Cloning, expression, and characterization of a nitric oxide synthase protein from Deinococcus radiodurans. Proc Natl Acad Sci U S A 99: 107-112.

90. Reece SY, Woodward JJ, Marletta MA (2009) Synthesis of nitric oxide by the NOS-like protein from deinococcus radiodurans: a direct role for tetrahydrofolate. Biochemistry 48: 5483-5491.

91. Patel BA, Moreau M, Widom J, Chen H, Yin L, et al. (2009) Endogenous nitric oxide regulates the recovery of the radiation-resistant bacterium Deinococcus radiodurans from exposure to UV light. Proc Natl Acad Sci U S A 106: 18183-18188.

92. Kers JA, Wach MJ, Krasnoff SB, Widom J, Cameron KD, et al. (2004) Nitration of a peptide phytotoxin by bacterial nitric oxide synthase. Nature 429: 79-82.

93. Hogenhout SA, Loria R (2008) Virulence mechanisms of Gram-positive plant pathogenic bacteria. Curr Opin Plant Biol 11: 449-456.

94. Gusarov I, Shatalin K, Starodubtseva M, Nudler E (2009) Endogenous nitric oxide protects bacteria against a wide spectrum of antibiotics. Science 325: 1380-1384.

95. Adak S, Aulak KS, Stuehr DJ (2002) Direct evidence for nitric oxide production by a nitric-oxide synthase-like protein from Bacillus subtilis. J Biol Chem 277: 16167-16171.

96. Gusarov I, Nudler E (2005) NO-mediated cytoprotection: instant adaptation to oxidative stress in bacteria. Proc Natl Acad Sci U S A 102: 13855-13860.

97. Bird LE, Ren J, Zhang J, Foxwell N, Hawkins AR, et al. (2002) Crystal structure of SANOS, a bacterial nitric oxide synthase oxygenase protein from Staphylococcus aureus. Structure 10: 1687-1696.

98. Chartier FJ, Couture M (2007) Substrate-specific interactions with the heme-bound oxygen molecule of nitric-oxide synthase. J Biol Chem 282: 20877-20886.

99. Salard I, Mercey E, Rekka E, Boucher JL, Nioche P, et al. (2006) Analogies and surprising differences between recombinant nitric oxide synthase-like proteins from Staphylococcus aureus and Bacillus anthracis in their interactions with l-arginine analogs and iron ligands. J Inorg Biochem 100: 2024-2033.

100. Lowy FD (1998) Staphylococcus aureus infections. N Engl J Med 339: 520-532.

101. Arvand M, Bhakdi S, Dahlback B, Preissner KT (1990) Staphylococcus aureus alpha-toxin attack on human platelets promotes assembly of the prothrombinase complex. J Biol Chem 265: 14377-14381.

102. Marrack P, Kappler J (1990) The staphylococcal enterotoxins and their relatives. Science 248: 1066.

103. Travis J, Potempa J, Maeda H (1995) Are bacterial proteinases pathogenic factors? Trends Microbiol 3: 405-407.

104. Gotz F, Verheij HM, Rosenstein R (1998) Staphylococcal lipases: molecular characterisation, secretion, and processing. Chem Phys Lipids 93: 15-25.

105. Holden MT, Feil EJ, Lindsay JA, Peacock SJ, Day NP, et al. (2004) Complete genomes of two clinical Staphylococcus aureus strains: evidence for the rapid evolution of virulence and drug resistance. Proc Natl Acad Sci U S A 101: 9786-9791.

106. Clewell DB, Flannagan SE, Jaworski DD (1995) Unconstrained bacterial promiscuity: the Tn916-Tn1545 family of conjugative transposons. Trends Microbiol 3: 229-236.

107. Groicher KH, Firek BA, Fujimoto DF, Bayles KW (2000) The Staphylococcus aureus lrgAB operon modulates murein hydrolase activity and penicillin tolerance. J Bacteriol 182: 1794-1801.

108. Shafer WM, Iandolo JJ (1979) Genetics of staphylococcal enterotoxin B in methicillin-resistant isolates of Staphylococcus aureus. Infect Immun 25: 902-911.

109. Schenk S, Laddaga RA (1992) Improved method for electroporation of Staphylococcus aureus. FEMS Microbiol Lett 73: 133-138.

110. Inoue H, Nojima H, Okayama H (1990) High efficiency transformation of Escherichia coli with plasmids. Gene 96: 23-28.

111. Brown T (2001) Southern blotting. Curr Protoc Protein Sci Appendix 4: Appendix 4G.

112. Morikawa K, Maruyama A, Inose Y, Higashide M, Hayashi H, et al. (2001) Overexpression of sigma factor, sigma(B), urges Staphylococcus aureus to thicken the cell wall and to resist beta-lactams. Biochem Biophys Res Commun 288: 385-389.

113. Heydorn A, Nielsen AT, Hentzer M, Sternberg C, Givskov M, et al. (2000) Quantification of biofilm structures by the novel computer program COMSTAT. Microbiology 146 (Pt 10): 2395-2407.

114. Yang SJ, Rice KC, Brown RJ, Patton TG, Liou LE, et al. (2005) A LysR-type regulator, CidR, is required for induction of the Staphylococcus aureus cidABC operon. J Bacteriol 187: 5893-5900.

115. Patton TG, Rice KC, Foster MK, Bayles KW (2005) The Staphylococcus aureus cidC gene encodes a pyruvate oxidase that affects acetate metabolism and cell death in stationary phase. Mol Microbiol 56: 1664-1674.

116. Chang W, Small DA, Toghrol F, Bentley WE (2006) Global transcriptome analysis of Staphylococcus aureus response to hydrogen peroxide. J Bacteriol 188: 1648-1659.

117. Gruber TM, Gross CA (2003) Multiple sigma subunits and the partitioning of bacterial transcription space. Annu Rev Microbiol 57: 441-466.

118. Kapanidis AN, Margeat E, Laurence TA, Doose S, Ho SO, et al. (2005) Retention of transcription initiation factor sigma70 in transcription elongation: single-molecule analysis. Mol Cell 20: 347-356.

119. Logan J, Edwards K, Saunders N, editors (2009) Real-time PCR: Current Technology and Applications. Norfolk, UK: Caister Academic Press.

120. (2006) Real-Time PCR Applications Guide. In: Bio-Rad Laboratories I, editor.

121. Bae T, Banger AK, Wallace A, Glass EM, Aslund F, et al. (2004) Staphylococcus aureus virulence genes identified by bursa aurealis mutagenesis and nematode killing. Proc Natl Acad Sci U S A 101: 12312-12317.

122. Miller WG, Lindow SE (1997) An improved GFP cloning cassette designed for prokaryotic transcriptional fusions. Gene 191: 149-153.

123. Hanahan D (1983) Studies on transformation of Escherichia coli with plasmids. J Mol Biol 166: 557-580.

124. Kreiswirth BN, Lofdahl S, Betley MJ, O'Reilly M, Schlievert PM, et al. (1983) The toxic shock syndrome exotoxin structural gene is not detectably transmitted by a prophage. Nature 305: 709-712.

125. Gillaspy AF, Hickmon SG, Skinner RA, Thomas JR, Nelson CL, et al. (1995) Role of the accessory gene regulator (agr) in pathogenesis of staphylococcal osteomyelitis. Infect Immun 63: 3373-3380.

126. Duthie ES, Lorenz LL (1952) Staphylococcal coagulase; mode of action and antigenicity. J Gen Microbiol 6: 95-107.

127. Dyke KG, Jevons MP, Parker MT (1966) Penicillinase production and intrinsic resistance to penicillins in Staphylococcus aures. Lancet 1: 835-838.

128. Charpentier E, Anton AI, Barry P, Alfonso B, Fang Y, et al. (2004) Novel cassette-based shuttle vector system for gram-positive bacteria. Appl Environ Microbiol 70: 6076-6085.

129. Bruckner R (1997) Gene replacement in Staphylococcus carnosus and Staphylococcus xylosus. FEMS Microbiol Lett 151: 1-8.

130. Lan L, Cheng A, Dunman PM, Missiakas D, He C (2010) Golden pigment production and virulence gene expression are affected by metabolisms in Staphylococcus aureus. J Bacteriol 192: 3068-3077.

131. Zhang S, Pohnert G, Kongsaeree P, Wilson DB, Clardy J, et al. (1998) Chorismate mutase-prephenate dehydratase from Escherichia coli. Study of catalytic and regulatory domains using genetically engineered proteins. J Biol Chem 273: 6248-6253.

132. Perera A, Parkes HG, Herz H, Haycock P, Blake DR, et al. (1997) High resolution 1H NMR investigations of the reactivities of alpha-keto acid anions with hydrogen peroxide. Free Radic Res 26: 145-157.

133. Zhang Y, Morar M, Ealick SE (2008) Structural biology of the purine biosynthetic pathway. Cell Mol Life Sci 65: 3699-3724.

134. Henard CA, Bourret TJ, Song M, Vazquez-Torres A (2010) Control of redox balance by the stringent response regulatory protein promotes antioxidant defenses of Salmonella. J Biol Chem.

BIOGRAPHICAL SKETCH

Erin Ahmo Almand is a Waterford, Connecticut native who graduated from Waterford High School in 2005. Upon graduation, she attended the United States Air Force Academy where she graduated in 2009 with a Bachelor of Science in biology and received a commission as a Second Lieutenant in the United States Air Force. After commissioning, she was picked for a scholarship to pursue a Master of Science degree by the Air Force Institute of Technology. She attended the University of Florida, and in December 2010, graduated with a Master of Science in microbiology. After graduation, Erin was sent to Eglin Air Force Base in Fort Walton Beach, Florida where she currently resides with her husband, Austin Almand.